

In Search of Lost Online Test-time Adaptation: A Survey

Zixin Wang · Yadan Luo · Liang Zheng · Zhuoxiao Chen · Sen Wang ·
Zi Huang

Received: date / Accepted: date

Abstract In this paper, we present a comprehensive survey on online test-time adaptation (OTTA), a paradigm focused on adapting machine learning models to novel data distributions upon batch arrival. Despite the proliferation of OTTA methods recently, the field is mired in issues like ambiguous settings, antiquated backbones, and inconsistent hyperparameter tuning, obfuscating the real challenges and making reproducibility elusive. For clarity and a rigorous comparison, we classify OTTA techniques into three primary categories and subject them to benchmarks using the potent Vision Transformer (ViT) backbone to discover genuinely effective strategies. Our benchmarks span not only conventional corrupted datasets such as CIFAR-10/100-C and ImageNet-C but also real-world shifts embodied in CIFAR-10.1 and CIFAR-10-Warehouse, encapsulating variations across search engines and synthesized data by diffusion models. To gauge efficiency in online scenarios, we introduce novel evaluation metrics, inclusive of FLOPs, shedding light on the trade-offs between adaptation accuracy and computational overhead. Our findings diverge from existing literature, indicating: (1) transformers exhibit heightened resilience to diverse domain shifts, (2) the efficacy of many OTTA methods hinges on ample batch sizes, and (3) stability in optimization and resistance to perturbations are critical during adaptation, especially when the batch size is 1. Motivated by these insights, we pointed out promising directions for future research. The source code will be made available.

Keywords Online Test-time Adaptation · Transfer Learning

School of Electrical Engineering and Computer Science
The University of Queensland, Australia
E-mail: {zixin.wang, y.luo, zhuoxiao.chen, sen.wang, helen.huang}@uq.edu.au, liang.zheng@anu.edu.au

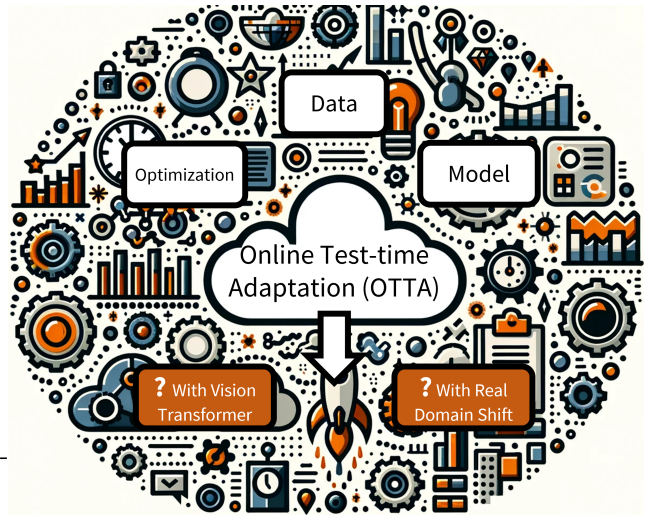


Fig. 1: An illustrative figure of our survey. We comprehensively summarized the advanced OTTA techniques under the categories of optimization, model, and data. The main research questions are: Is OTTA still effective when (1) integrated with Vision Transformer? (2) encountered with real-world domain shift?

1 Introduction

The presence of dataset shift (Quinero-Candela et al. 2008) poses a notable challenge for machine learning. Models often experience significant performance drop when they confront test data characterized by conspicuous *distribution differences* from training. Such differences might come from changes in style and lighting conditions, and various forms of corruption, making test data deviate from the data upon which these models were initially trained. To mitigate the performance degradation during inference, test-time adapta-

tion (TTA) has emerged as a promising solution. TTA aims to rectify the dataset shift issue by acclimating the model to novel distributions using unlabeled test data (Liang et al. 2023). Different from the traditional paradigm of domain adaptation (Ganin and Lempit-sky 2015; Wang and Deng 2018), TTA does not require access to source data for distribution alignment. Commonly used strategies in TTA include unsupervised proxy objectives, spanning techniques such as pseudo-labeling Liang et al. (2020), graph-based learning (Luo et al. 2023), and contrastive learning Chen et al. (2022a), applied across the **entire expanse** of test data through multiple training epochs to enhance model accuracy. Nevertheless, requiring access to the complete test set may not always align with practical use. In many applications such as object detection, adaptation is restricted to using only the **current test batch** processed in a streaming manner. Such operational restrictions make it untenable for TTA to require the full test set tenable.

In this study, our focus is on a specific line of TTA methods, *i.e.*, online test-time adaptation (OTTA), which aims to accommodate *real-time changes* in the test data distribution. We provide a comprehensive overview of existing OTTA studies and evaluate the efficiency and effectiveness of its individual components. To facilitate a structured comprehension of the OTTA landscape, below we categorize existing approaches into three groups: data-centric OTTA, model-based OTTA, and optimization-oriented OTTA.

- **Data-centric OTTA** maximizes prediction consistency across diversified test data. Diversification strategies use auxiliary data, improved data augmentation methods, and diffusion techniques, and create a saving queue for test data, *etc.*
- **Model-based OTTA** makes changes to the original backbone, such as modifying specific layers or their mechanisms, adding supplementary branches, and incorporating prompts.
- **Optimization-oriented OTTA** focuses on various optimization methods. Examples are designing new loss functions, updating **BatchNorm** layers during testing, using pseudo-labeling strategies, teacher-student frameworks, and contrastive learning-based approaches, *etc.*

It is potentially useful to combine methods from different categories for further improvement. An in-depth analysis on this strategy is presented in Section 3.

Differences from an existing survey. Liang et al. (2023) provides a comprehensive overview of the vast topic of test-time adaptation (TTA), discussing TTAs in diverse configurations and their applicability in vision, natural language processing (NLP), and graph

data analysis. One limitation is that the survey does not provide experimental comparisons of existing methods. In comparison, our survey focuses on online TTA methods and provides interesting insights from experimental comparisons with consideration in hyperparameter selection and backbone influence (Zhao et al. 2023b). **Contributions.** In particular, with the ascent of vision transformer (ViT) architectures in various machine learning domains, this survey studies *whether OTTA strategies developed for ResNet structures maintain their effectiveness after being integrated into ViT instead*. To this end, we benchmark seven state-of-the-art OTTA algorithms on a wide range of distribution shifts under a new set of evaluation metrics. Below, we summarize the key contribution of this survey.

- **[A focused OTTA survey]** To the best of our knowledge, this is the first focused survey on online test-time adaptation, which provides a thorough understanding of three main working mechanisms. Wide experimental investigations are conducted in a fair comparison setting.
- **[Benchmarking OTTA strategies with ViT]** We reimplemented representative OTTA baselines under the ViT architecture and testified their performance against five benchmark datasets. We drive a set of replacement rules that adapt the existing OTTA methods to accommodate the new backbone.
- **[Both accuracy and efficiency as evaluation Metrics]** Apart from using the traditional recognition accuracy metric, we further provide insights into various facets of computational efficiency by Giga floating-point operations per second (GFLOPs). These metrics are important in real-time streaming applications.
- **[Real-world testbeds]** While existing literature extensively explore OTTA methods on corruption datasets like CIFAR-10-C, CIFAR-100-C, and ImageNet-C, our interests are more fall into their capability to navigate real-world dataset shifts. Specifically, we assess OTTA performance on CIFAR-10-Warehouse, a newly introduced, expansive test set of CIFAR10. Our empirical analysis and evaluation lead to different conclusions from findings in the existing survey (Liang et al. 2023).

This work aims to summarize the numerous OTTA methods with the aforementioned three categorization criteria and analyze each approach using empirical results. Moreover, to assess real-world potential, we conduct comparative experiments to explore the portability, robustness, and environment sensitivity of the OTTA components. We expect this survey to offer a systematic perspective in navigating OTTA’s intricate and diverse settings, enabling a clear identification of

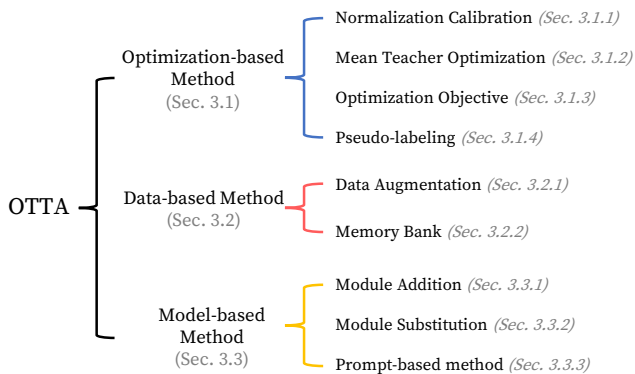


Fig. 2: Taxonomy of existing OTTA methods. The categories, i.e., optimization-based, data-based, and model-based, inform three mainstream working mechanisms. Additional smaller categories are based on prompt tuning and input adaptation.

effective components. We also present new challenges as potential future research directions.

Organization of the survey. The rest of this survey will be organized as follows. Section 2 presents the problem definition and introduces widely used datasets, metrics and applications. Using the taxonomy shown in Fig. 2, Section 3 provides a comprehensive review of existing OTTA methods. Then, using transformer backbones, Section 4 empirically analyzes seven state-of-the-art methods based on a set of new evaluation metrics on both corrupted and real-world distribution shifts. We conclude the survey in Section 6.

2 Problem Overview

Online Test-time Adaptation (OTTA), with its online and on-time characteristics, represent a critical line of methods in test-time adaptation. This section provides a formal definition of OTTA and delves into its fundamental attributes. Further, we explore widely used datasets and evaluation methods and examine the potential application scenarios of OTTA. To ensure a clear understanding, A comparative analysis is undertaken to differentiate OTTA from other settings that bear resemblance.

2.1 Problem Definition

In OTTA, we assume access to a trained source model and adapt the model at test time over the test input before making the final prediction. The given source model f_{θ^S} parameterized by θ^S is pre-trained on a labeled source domain $\mathcal{D}_S = \{(\mathbf{x}^S, \mathbf{y}^S)\}$, which is formed by i.i.d. sampling from the source distribution p_S . Unlabeled test data come in batches: $\mathcal{D}_T = \{\mathbf{x}_1^T, \mathbf{x}_2^T, \mathbf{x}_i^T, \dots, \mathbf{x}_n^T\}$,

where t indicates the time step. Test data often come from one or multiple different distributions $(\mathbf{x}_i^T, \mathbf{y}_i^T) \sim p_T$, where $p_S(\mathbf{x}, \mathbf{y}) \neq p_T(\mathbf{x}, \mathbf{y})$ under the covariate shift assumption (Huang et al. 2006). During TTA, we update the model parameters at each time step, resulting in an adapted model f_{θ^t} . The pre-trained model is expected to retain its original architecture, including the backbone, without modifying its layers or introducing new model branches during training. Additionally, the model is restricted to observing the test data only once and must produce predictions promptly. By refining the definition of OTTA in this manner, we aim to minimize limitations associated with its application in real-world settings. Note that following adaptation to a specific domain, the model is reset to its original pretrained state. *i.e.*, $f_{\theta^S} \rightarrow f_{\theta^0} \rightarrow f_{\theta^S} \rightarrow f_{\theta^1} \rightarrow f_{\theta^S} \rightarrow \dots f_{\theta^t}$.

Due to the covariate shift between the source and test data, adapting the source model in the absence of the source data poses a significant challenge. Since there is no way to align these two sets together, one may ask, what kind of optimization objective could work under such a limited environment? Meanwhile, as the test data come at a fixed pace, how many of them could be a desirable amount to best fix the test-time adaptation? Or even, will the adaptation still work in the new era of backbones (e.g., ViTs)? Does “Test-time Adaptation” become a false proposition with the backbone upgrading? With these concerns, we unfold the OTTA methods by their datasets, evaluations, and applications and decouple their strategies, aiming to discover which one and why one component would work with the update of existing backbones.

2.2 Datasets

This survey mainly summarizes datasets in image classification, a fundamental problem in computer vision, while recognizing that OTTA has been applied to many downstream tasks (Ma et al. 2022; Ding et al. 2023; Saltori et al. 2022). Testbeds in OTTA usually seek to facilitate adaptation from natural images to corrupted ones. The latter are created by perturbations such as Gaussian noise and defocus blur. Despite the inclusion of corruptions at varying severities, these synthetically induced corruptions may not sufficiently mirror the authentic domain shift encountered in real-world scenarios. In our work, we use both corruption and real-world shift datasets, summarized in Table 1. Details of each testbed are described below.

- **CIFAR-10-C** is a standard benchmark for image classification. It contains 60,000 color images, each

Table 1: **Datasets used in this survey.** We list their key statistics.(Sun et al. 2023) Note that only a subset of each below datasets will be used.

Datasets	# domains	# test images	# classes	corrupted?	image size
CIFAR-10-C (Hendrycks and Dietterich 2018)	19	950,000	10	Yes	32×32
CIFAR-100-C (Hendrycks and Dietterich 2018)	19	950,000	100	Yes	32×32
ImageNet-C (Hendrycks and Dietterich 2018)	75	3750,000	1000	Yes	224×224
CIFAR-10.1 (Recht et al. 2018)	1	2,000	10	No	32×32
CIFAR-10-Warehouse (Sun et al. 2023)	180	608,691	10	No	224×224

10 Corrupted retains the class structure of CIFAR10 but incorporates 15 diverse corruption styles, with severities ranging from levels 1 to 5. This corrupted variant aims to simulate realistic image distortions or corruptions that might arise during processes like image acquisition, storage, or transmission.

- **CIFAR-100-C** has 60,000 colored images with dimensions 32×32 pixels, uniformly distributed across 100 unique classes, resulting in 600 images per class. The CIFAR100 Corrupted dataset, analogous to CIFAR10 Corrupted, integrates artificial corruptions into the canonical CIFAR100 images.
- **ImageNet-C** is a corrupted version of ImageNet 1k (Krizhevsky et al. 2012).

While testbest with corruptions have been widely used, they represent artificially created domain differences that may not fully capture the complexities in real-world scenarios. In fact, experimental benchmarking in this context is still lacking. Hence, this paper also evaluates OTTA on real-world test sets including CIFAR-10-Warehouse and CIFAR10.1 to address this limitation.

- **CIFAR-10.1** (Recht et al. 2018) is an out-of-distribution test set with the same label space as CIFAR10. It contains roughly 2,000 images sampled from Tiny Image dataset (Yang et al. 2016).
- **CIFAR-10-Warehouse** (CIFAR-10-W) integrates images from both diffusion models, specifically Stable-diffusion-2-1 (Rombach et al. 2022), and targeted keyword searches across seven popular search engines. Comprising 37 generated and 143 real-world datasets, each subset has 300 to 8,000 images, revealing noticeable within-class variations across different search criteria.

2.3 Evaluation

For online test-time adaptation, efficiency is an important consideration besides accuracy. This survey uses the following evaluation metrics.

Mean error (mErr) is one of the most commonly used metrics to assess model accuracy. It computes the

average error rate across all corruption types or domains. irrespective of the class to which the data points belong. The formula for calculating the mean error is given as:

$$\text{mErr} = \frac{1}{n} (1 - \text{acc}), \quad (1)$$

where n is the number of test domains, and acc represents model accuracy. While being useful most of the time, this metric does not provide class-specific insights, which might be important in some applications.

Floating point operations per second (FLOPS) quantifies the number of floating-point calculations a model performs in a second. A model with lower FLOPS is more computationally efficient.

Number of updated parameters provides insights into the complexity of the adaptation process. A model that requires a large number of parameters may not be practical for online adaptation.

2.4 Applications

OTTA is applied in a wide range of tasks such as autonomous vehicle detection (Hegde et al. 2021), pose estimation (Lee et al. 2023), video depth prediction (Liu et al. 2023), and frame interpolation (Choi et al. 2021). Regarding medical diagnosis, there is also a high demand for diagnostic models trained on a specific group of patient data to be adapted to new data (Ma et al. 2022; Wang et al. 2022b; Saltori et al. 2022).

2.5 Relationship with Other Tasks

Offline test-time adaptation (TTA), also called source-free domain adaptation, is a technique to adapt a source pre-trained model to the target (*i.e.*, test) set. This task assumes that the model can access the entire dataset. This differs from online test-time adaptation, where the test data is given in batches.

Continual TTA While OTTA requires resetting the adapted model back to the source pre-trained one for every distinct corruption type, continual TTA (*e.g.*,

(Wang et al. 2022a)) does not allow any reset mechanism if it is based on prior domain information.

Gradual TTA tackles real-world scenarios where domain shifts are gradually introduced through incoming test samples (Marsden et al. 2022). An example is the gradual and continuous change in weather conditions. For corruption datasets, existing gradual TTA approaches assume that test data transition from severity level 1 to level 2, and then progress slowly towards the highest level. Note that both continual and gradual TTA methods could also support online episodic learning.

Test-time Training (TTT) introduces an auxiliary task for both training and adaptation (Sun et al. 2020; Gandelsman et al. 2022). In the training phase, the original architecture, such as ResNet101, is modified into a “Y”-shaped structure, where one task is image classification, and the other could be rotation prediction. During adaptation, the auxiliary task continues to be trained in a supervised manner so that model parameters are updated. The classification head output serves as the final prediction for each test sample.

Test-time augmentation (TTAug) applies data augmentations to input data during inference, resulting in multiple variations of the same test sample, from which predictions are obtained (Shanmugam et al. 2021; Kimura 2021). The final prediction typically aggregates predictions of these augmented samples through averaging or majority voting. TTAug enhances model robustness and generalization by providing a range of data views. This technique can be applied to various tasks, including domain adaptation, offline TTA, and even OTTA. TTAug and TTA are fundamentally incomparable as they pertain to distinct methodologies.

Domain generalization aims to train models that can perform effectively across multiple distinct domains without specific adaptation to any domain (Zhou et al. 2023). It assumes the model learns domain-invariant features that are applicable across diverse datasets. While OTTA emphasizes dynamic adaptation to specific domains over time, domain generalization seeks to establish domain-agnostic representations. The choice between these strategies depends on the specific problem considered.

3 Online test-time adaptation

Given the divergence of online data from the distribution of source training data, OTTA techniques are broadly classified into three categories. These categorizations hinge on their responses to two primary concerns: managing online data and mitigating performance

drops due to distribution shifts. Optimization-centric methods anchored in designing unsupervised objectives typically lean towards adjusting or enhancing pre-trained models. **Model-centric** approaches look to modify particular layers or even overhaul the architecture. On the other hand, **data-centric** methods aim to expand data diversity, either to amplify model generalization or to harmonize consistency across varying data views. According to this taxonomy, we sort out existing approaches in Table ?? and review them in detail as follows.

3.1 Optimization-based OTTA

Optimization-based OTTA methods consist of three sub-categories: (1) recalibration statistics in normalization layers, (2) enhancing optimization stability with the mean-teacher model, and (3) designing unsupervised loss functions. A timeline is illustrated in Fig. 3.

3.1.1 Normalization Calibration

In deep learning, a normalization layer refers to a specialized architectural component that is integrated within neural network architectures. Its primary function is to ameliorate the training process and enhance the generalization capacity of deep neural networks by regulating the statistical properties of activations within a given layer. These layers, which include Batch Normalization (BatchNorm) (Ioffe and Szegedy 2015), Layer Normalization LayerNorm (Ba et al. 2016), and Instance Normalization (Ulyanov et al. 2016), among others, operate by standardizing the mean and variance of activations, thereby diminishing the likelihood of vanishing or exploding gradients during the training process. A similar idea of the normalization layer is feature whitening, which also adjusts the feature right after the activation layer. Both of them are commonly used in domain adaptation tasks to alleviate domain shift (Roy et al. 2019; Carlucci et al. 2017).

Example. Take the most commonly used BatchNorm as an example. Let \mathbf{x}_i represent the activation for feature channel i in a mini-batch. The BatchNorm layer will first calculate the batch-level mean $\boldsymbol{\mu}$ and variance $\boldsymbol{\sigma}^2$ by:

$$\boldsymbol{\mu} = \frac{1}{m} \sum_{i=1}^m \mathbf{x}_i, \quad \boldsymbol{\sigma}^2 = \frac{1}{m} \sum_{i=1}^m (\mathbf{x}_i - \boldsymbol{\mu})^2, \quad (2)$$

where m is the mini-batch size. Then, the calculated statistics will be applied to standardize the inputs:

$$\hat{\mathbf{x}}_i = \frac{\mathbf{x}_i - \boldsymbol{\mu}}{\sqrt{\boldsymbol{\sigma}^2 + \epsilon}}, \quad \mathbf{y}_i = \gamma \hat{\mathbf{x}}_i + \beta, \quad (3)$$

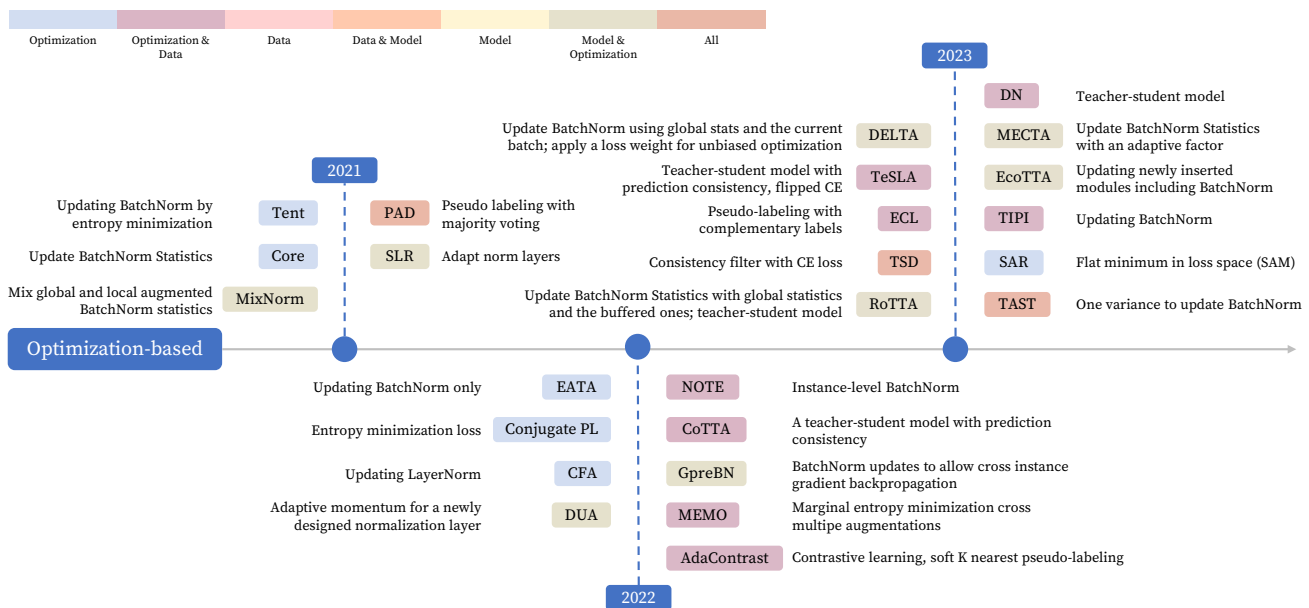


Fig. 3: Timeline of optimization-based OTTA methods.

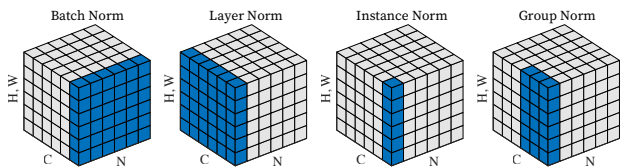


Fig. 4: Comparisons among different normalization layers (Wu and He 2020).

where y_i is the final output of the i -th channel from this batch normalization layer, with the adjustment of two learnable affine parameters, γ , and β . For the update, the running mean μ^{run} and variance σ^{run} are computed as a moving average (EMA) of the mean and variance over all batches seen during training, with a momentum factor α :

$$\mu^{\text{run}} = \alpha\mu + (1-\alpha)\mu^{\text{run}}, \quad \sigma^{\text{run}} = \alpha\sigma + (1-\alpha)\sigma^{\text{run}} \quad (4)$$

Motivation. In the case of domain adaptation, aligning batch normalization statistics has been proven to mitigate the performance degradation brought by covariate shifts. The hypothesis suggests that information pertaining to labels is encoded within the weight matrices of each layer, while knowledge related to specific domains is conveyed through the statistics of BatchNorm layer. Consequently, we can seamlessly adapt the pre-trained model to a different domain by adjusting the statistics within the BN layer (Li et al. 2017). Similar ideas can be borrowed in online test-time adaptation.

Assumption 1 (Normalization Calibration OTTA)

Given a neural network f trained on a source dataset \mathcal{D}_S with **normalization parameters** β and γ , updating $\{\gamma, \beta\}$ based on the test data x_i^T at each time step t will bolster f 's robustness on the corresponding domain.

Building upon Assumption 1, initial investigations in OTTA predominantly revolved around fine-tuning a designated loss function, focusing on updating the normalization layers exclusively. This deliberate approach was employed to mitigate the performance degradation resulting from shifts in data distributions, thereby ensuring the preservation of the fundamental learned representations of the pre-trained model. Within this overarching strategy, several discernible variations can be observed. A common practice entails the adjustment of statistics and affine parameters within the BatchNorm layer while leaving other model parameters unchanged. Additionally, the choice of normalization techniques, such as LayerNorm or GroupNorm, may vary based on architectural intricacies and specific optimization objectives. Furthermore, selecting appropriate loss functions may differ, reflecting distinct optimization goals.

Tent (Wang et al. 2021), and its subsequent endeavors, such as (Niu et al. 2022; Jang et al. 2023), are representative approaches within this paradigm. They expedited model adaptation to the current batch data by concentrating on the statistics of the batch at hand and exclusively updating the affine parameters of Batch Normalization. However, the effectiveness of batch-level updates, as seen in Tent, is contingent upon data quality within each batch, introducing potential performance

fluctuations. For example, the noise data or poisoned data with extremely biased statistics will significantly influence the `BatchNorm` statistics. To mitigate potential performance instability arising from batch-level statistics, a line of advanced techniques has been proposed: **Stabilization via Dataset-level Estimate**. Gradient Preserving Batch Normalization `GpreBN` (Yang et al. 2022) is proposed to allow cross instance gradient backpropagation by modifying the `BatchNorm` standardization:

$$\hat{\mathbf{y}}_i = \frac{\frac{\mathbf{x}_i - \boldsymbol{\mu}_c}{\boldsymbol{\sigma}_c} \bar{\boldsymbol{\sigma}}_c + \bar{\boldsymbol{\mu}}_c - \boldsymbol{\mu}}{\boldsymbol{\sigma}} \gamma + \beta \quad (5)$$

where $\frac{\mathbf{x}_i - \boldsymbol{\mu}_c}{\boldsymbol{\sigma}_c}$ is the standardized input feature $\hat{\mathbf{x}}_i$ as in Eq. (3). `GpreBN` further normalizes $\hat{\mathbf{x}}_i$ by stopping gradient backpropagation $\bar{\boldsymbol{\mu}}_c$ $\bar{\boldsymbol{\sigma}}_c$ and arbitrary non-learnable parameters $\boldsymbol{\mu}$ and $\boldsymbol{\sigma}$. `MixNorm` (Hu et al. 2021) introduces mixing up the statistics (produced by the augmented sample inputs) of the current batch with the global-level statistics by EMA. Then, the combined information from both historical and augmented batch-level statistics could effectively bridge the gap between historical context and real-time fluctuations, enhancing model performance. Exploring this line of research has led to alternative proposals, such as `RBN` (Yuan et al. 2023b), which considers global robust statistics from a well-maintained memory bank with a fixed momentum of EMA when updating statistics, to ensure a good statistic quality. `Core` (You et al. 2021) incorporate the mixup factor and introduce strategies to fuse source and test set statistics, reinforcing model discriminability.

Stabilization via Dynamic Momentum. The primary focus of the following works centers on the ratio at which historical and current statistics are combined. Instead of adhering to a fixed momentum factor for EMA, as suggested by `DUA` (Mirza et al. 2022), a dynamic approach is adopted. This dynamic approach determines the momentum based on a decay factor. Operating under the assumption that the model’s performance deteriorates over time, the decay factor should progressively incorporate more information from the current batch as time advances to avoid severe biased learning by low-quality `BatchNorm` updates. Consequently, this mitigates noise accumulation and its adverse impact on adaptation.

Stabilization via Renormalization. Nonetheless, an exclusive emphasis on moving averages might undermine the inherent characteristics of gradient optimization and normalization when it comes to updating `BatchNorm` layers. As previously noted by (Huang et al. 2018), `BatchNorm` primarily standardizes activations, centering and scaling them without addressing their correlations. In contrast, the Test-time Batch Renormalization

(TBR) in `DELTA` (Zhao et al. 2023a) addresses this limitation through a renormalization process involving the adjustment of standardized outputs using two newly introduced parameters, denoted as r and d . $r = \frac{sg(\bar{\boldsymbol{\sigma}}^{\text{batch}})}{\bar{\boldsymbol{\sigma}}^{\text{ema}}}$ and $d = \frac{sg(\bar{\boldsymbol{\mu}}^{\text{batch}}) - \bar{\boldsymbol{\mu}}^{\text{ema}}}{\bar{\boldsymbol{\sigma}}^{\text{ema}}}$, where $sg(\cdot)$ is stop gradient. Then $\hat{\mathbf{x}}_i$ is normalized further by $\hat{\mathbf{x}}_i = \hat{\mathbf{x}}_i \cdot r + d$. These parameters are computed using batch and global moving statistics, ushering in a novel approach to maintaining stable batch statistics updating strategies (inspired by (Ioffe 2017)). While the above methods are based on OTTA under the allowance of resetting the model for each domain, it limits the model to be applied to real-world scenarios that commonly have no domain information. `NOTE` (Gong et al. 2022), focusing on dealing with continual OTTA under temporal correlation (i.g., distribution changes over time t : $(\mathbf{x}_t, \mathbf{y}_t) \sim P_{\mathcal{T}}(\mathbf{x}, \mathbf{y} | t)$), proposes instance-level `BatchNorm` to avoid potential instance-wise variations in a domain non-identifiable paradigm.

Stabilization via Enlarge Batches. To ensure the stability of adaptation, an essential factor is utilizing large batch sizes. This is because including a greater volume of statistical data from a larger batch contributes to the robustness of the overall statistical information. Consequently, it is notable that nearly all methods based on Batch Normalization (`BatchNorm`) employ substantial batch sizes, for instance, setting the batch size to 200 when dealing with the CIFAR10 corrupted dataset. However, this practice can impose limitations on OTTA, particularly when dealing with scenarios where data arrives in smaller quantities due to hardware constraints, such as GPU memory limitations, especially in edge devices.

Alternatives to Batchnorm. To avoid using large batch size, updating `GroupNorm` (Mummadi et al. 2021) could benefit the adaptation. `LayerNorm` could also be one option, especially in transformer-based tasks (Kojima et al. 2022). At the same time, the batch-agnostic norm layer `LayerNorm` (as Fig.4 shows) is proved to be a solution of unstable adaptation under the assistance of sharpness-aware entropy minimization (Niu et al. 2023). Followed by the above situation in scenarios where computational resources are limited, `MECTA` (Hong et al. 2023) introduced an innovative approach by replacing the conventional `BatchNorm` layer with a customized `MECTA` norm. This strategic change effectively mitigated memory usage concerns during adaptation, reducing the memory overhead typically associated with large batch sizes, extensive channel dimensions, and numerous layers requiring updates. Taking a different tack, `EcoTTA` (Song et al. 2023) incorporated and exclusively updated meta networks, including `BatchNorm` layers.

This approach also effectively curtailed computational expenses while upholding robust test-time performance. Furthermore, to address the performance challenges associated with smaller batch sizes, TIPI (Nguyen et al. 2023) introduced additional `BatchNorm` layers in conjunction with the existing ones. This configuration inherently maintains two distinct sets of data statistics and leverages shared affine parameters to enhance consistency across different views of test data.

3.1.2 Mean Teacher Optimization

As mentioned in the previous subsection, stability in optimization is a core question to study. In the realm of OTTA, the Mean Teacher Model (Tarvainen and Valpola 2017) stands out as a formidable strategy. Central to the Mean Teacher framework is the incorporation of a consistency loss. This loss narrows the gap between the predictions of two intertwined models: the student and the teacher. Notably, the parameters of the teacher model θ_t are derived as an exponential moving average (EMA) of those of the student model θ_s , where the student model is initialized by source pre-trained weights θ^S . A foundational assumption underpinning this approach is the principle of **consistency regularization**. It posits that the resultant outputs should manifest congruence when two perturbed versions of the same input — whether modified through data augmentation or noise introduction — are processed through the model.

In light of the foregoing discussion, integrating the mean-teacher model within the context of OTTA, coupled with incorporating data-driven (Section 3.2) or model-driven (Section 3.3) methodologies, holds the promise of enhancing the stability of predictions. This heightened stability arises from the model’s reduced sensitivity to diverse augmented perspectives of unlabeled test data, potentially engendering favorable characteristics derived from other constituent components within the comprehensive framework.

Divergence in Updating Strategies. CoTTA (Wang et al. 2022a) is a representative method under the mean-teacher framework, which employs a conventional updating strategy that hinges on consistency loss between strongly and weakly augmented data samples drawn from the teacher and student networks. To determine which layers to update and avoid catastrophic forgetting, CoTTA incorporates a **stochastic parameter reset** strategy. This strategy involves utilizing a predetermined reset factor, whereby the model selectively and randomly resets a fixed number of parameters to their source pre-trained states in each iteration. This precautionary measure aids in preserving the model’s learned

knowledge while guarding against the potentially detrimental consequences of misinformed updates. Furthermore, in terms of generating different views of test data, CoTTA employs commonly utilized data augmentation techniques, including adjustments in contrast, brightness, and other relevant transformations, to create strongly augmented views. In contrast to CoTTA’s updating rules, RoTTA (Yuan et al. 2023b) adopts a distinct updating strategy. Specifically, RoTTA focuses its model updates solely on the customized Batch Normalization layer (RBN) within the student model rather than modifying all parameters of the student model indiscriminately. This strategy serves a dual purpose: firstly, it allows RoTTA to harness the advantages of consistency regularization, and secondly, it also bolsters the model’s capacity to effectively manage out-of-distribution data by integrating distribution statistics into its learning process.

Divergence in Augmentations. Drawing inspiration from the teacher-student knowledge distillation, TeSLA (Tomar et al. 2023) aims to improve the student model’s performance on challenging (high entropy) test images. To achieve this, they advocate for the use of augmentations adversarial to the current teacher model, which act as a means to emulate images in the feature space’s uncertain areas. The model is subsequently refined by the student’s update to bridge the consistency gap between predictions on these high entropy augmented images and their corresponding soft-pseudo labels from non-augmented counterparts. As a result, the model undergoes self-distillation on “Easy” test images possessing confident soft-pseudo labels. Conversely, updates based on “Hard” test images are omitted, which enhances the separation of features on a class-by-class basis.

3.1.3 Optimization Objective

Designing a proper optimization objective is half the success of learning a good machine learning model. However, it turns hard in the scenario of test-time adaptation under limited information availability. Commonly used objectives for OTTA are summarized in Figure 5. Previous papers tend to solve the OTTA problem by considering three main challenges.

Uncertainty Reduction: A covariate shift can significantly impair the performance of source models on test samples. When a model yields highly uncertain predictions, it signals a lack of confidence, reflecting a potential misalignment with the novel data distribution. Continuous high uncertainty across successive test data denotes the model cannot capture the nuances of the new data representation. In light of these considera-

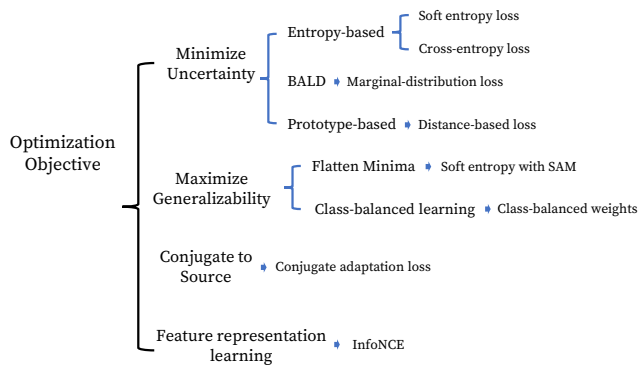


Fig. 5: Common optimization objectives in OTTA.

tions, the fundamental aim of Online Test-time Adaptation (OTTA) becomes evident: to instill confidence in the model’s predictions for test data in an online and unsupervised manner.

Entropy-based uncertainty: Shannon entropy (Shannon 1948), in the form of

$$H(\hat{y}) = - \sum_c p(\hat{y}_c) \log p(\hat{y}_c), \quad (6)$$

is originally designed for information theory. Its basic idea is that the “informational value” of a communicated message depends on the degree to which the content of the message is surprising. If a highly likely event occurs, the message carries very little information. On the other hand, if a highly unlikely event occurs, the message is much more informative. By this intuition, entropy minimization is borrowed in OTTA. While no labeled data exist during adaptation, reducing its entropy could make the model certain for predicting the current data sample.

Tent (Wang et al. 2021), as the representative of this stream, using the soft entropy in Eq. (6) to update the **BatchNorm** layers (Sec. 3.1.1) in an online manner. Its overall objective aims to fit the model to the test data by 1). reducing uncertainty (i.e., encouraging high prediction confidence) and 2). updating the **BatchNorm** layer to suit the test data distribution without label information. Follow-up works adopt a similar strategy, including **EATA** (Niu et al. 2022) which uses a sample selection score as the weight to measure if one sample is reliable and not redundant, **TTPR** (Sivaprasad et al. 2021), which combines entropy minimization with a consistency loss across different views of the test image, and, **SAR** (Niu et al. 2023), which explicitly considers to seeking for a flat minimum as in Eq. (8) for optimization when updating the model by the soft entropy.

While entropy minimization seems a satisfactory solution for OTTA, it raises some issues: instability and early convergence. This makes the prediction may fall

into biases. **SLR** (Mummadi et al. 2021) proposes to tackle these issues by replacing the entropy with a non-saturating surrogate and adding a diversity regularizer based on batch-wise entropy maximization that prevents convergence to trivial collapsed solutions. **SLR** proposes to minimize the negative log-likelihood ratio between classes rather than focusing on minimizing entropy loss. To encourage the diverse prediction, the diverse regularizer (i.e., KL divergence between model prediction distribution with a uniform distribution) is then applied and combined with the non-saturating surrogate.

The cooperation between a teacher and a student offers yet another realm for exploration. **PETAL**, **CoTTA**, and **RoTTA** (Yuan et al. 2023b) employs the cross-entropy loss, where the teacher’s outputs supervise the student’s predictions. Meanwhile, **RoTTA** further considers the age of the samples to be updated in the memory bank as a weight of the loss, making the model prefer to learn more about the newly added data samples in the memory bank. This further avoids the model (biased) overfitting to the old samples in the memory bank. Similarly, **PETAL** uses cross-entropy in its mean-teacher framework

Bayesian Active Learning by Disagreements (BALD):

Bayesian Active Learning (Bayesian AL) offers a comprehensive probabilistic perspective on estimating model uncertainty (Cao and Tsang 2021). In essence, Bayesian AL aims to maximize information gain by assessing predictive entropy, leading to the concept of Bayesian active learning by disagreements (BALD). BALD, in its essence, focuses on two primary aspects: estimating model uncertainty and constructing coresets (Campbell and Broderick 2018). A greedy approach is often employed to evaluate a model’s uncertainty, targeting data points that highlight discrepancies between a model’s current parameters and subsequent updates. BALD could identify the high uncertainty (or disagreement) sample in online test-time adaptation. By focusing on these samples, the model will likely make more meaningful updates that address the underlying shift in the test data distribution. One classical method that falls into this category is **MEMO** (Zhang et al. 2022). It proposes to adapt the model using the entropy of its marginal output distribution over augmentations. It aims to match the individual sample distribution with the expected distribution estimated by Monte Carlo dropout. By integrating the concept of BALD with multiple data augmentations, **MEMO** sets out to accomplish two primary objectives: first, to ensure the model will optimize the uncertainty and informative samples by aligning with expected marginal distribution, and thus, to bolster the

model’s confidence in its predictions by reducing the uncertainty.

Similarly, TeSLA borrows the concept of BALD to design its objective: the soft pseudo-label loss, wherein the student’s output provides the supervision feedback. Minimizing this loss between the student model’s predictions and the soft pseudo-labels — combined with the negative entropy of its marginalized predictions over test images — can be interpreted as mutual information maximization. The overall objective could be seen as follows:

$$\begin{aligned} \mathcal{L}_{\text{pl}}(\mathbf{X}, \hat{\mathbf{Y}}) = & -\frac{1}{B} \sum_{i=1}^B \sum_{k=1}^K f_s(\mathbf{x}_i)_k \log((\hat{\mathbf{y}}_i)_k) \\ & + \sum_{k=1}^K \hat{f}_s(\mathbf{X})_k \log(\hat{f}_s(\mathbf{X})_k), \end{aligned} \quad (7)$$

where $\hat{f}_s(\mathbf{X}) = \frac{1}{B} \sum_{i=1}^B f_s(\mathbf{x}_i)$ is the marginal class distribution over the batch. This could, as well, enable the model to focus more on the “useful” data and enhance the prediction confidence at the same time.

Prototype-based Optimization: In OTTA, where the absence of test labels poses a challenge, prototype-based learning emerges as a commonly employed strategy to mitigate the impact of potentially noisy predictions. While common methods are solely based on the source-trained linear classifier, this, instead, shifts the focus to predicting labels in accordance with class prototypes. In recent developments, exemplified by TSD (Wang et al. 2023), the emphasis lies in guiding test data features towards their closest prototypes while preserving the uniformity of predictions. To achieve this, the prediction for test data is determined by measuring the cosine similarity between the feature representation of the test data and the corresponding prototype. A Shannon entropy-based filter is introduced to counteract noisy predictions during the initial model adaptation phase. In addition, since the predictions from different classifiers should be consistent, a new filter is designed. This consistency filter allows model optimization only when predictions exhibit consistency, thereby reducing noisy labels’ influence.

Maximize Generalizability: Generalizability, in the context of machine learning, refers to a model’s capability to perform effectively on new, previously unobserved data, regardless of its distribution. In the context of OTTA, this concept can be extended to entail the adaptation of the model, not only to perform well on the current data samples but also to ensure its readiness for forthcoming test samples.

To enhance the generalization capacity, inspired by Sharpness-aware Minimization (SAM) (Foret et al. 2021), SAR (Niu et al. 2023) formulates its objectives to find

out the flat minima to avoid violent fluctuations during optimization:

$$\min_{\Theta} S(\mathbf{x}) E^{SA}(\mathbf{x}; \Theta) \quad (8)$$

Here, $S(\mathbf{x})$ represents an entropy-based indicator function that filters out unreliable predictions based on a predefined threshold. Additionally, $E^{SA}(\mathbf{x}; \Theta)$ is defined as:

$$E^{SA}(\mathbf{x}; \Theta) \triangleq \max_{\|\epsilon\|_2 \leq \rho} E(\mathbf{x}; \Theta + \epsilon) \quad (9)$$

This term aims to identify a weight perturbation ϵ within a Euclidean ball of radius ρ that maximizes entropy. It quantifies sharpness by measuring the maximal change in entropy between Θ and $\Theta + \rho$. The ultimate objective involves the joint minimization of entropy and sharpness of entropy loss, creating a bi-level optimization problem that encourages the discovery of flat minima and bolsters the model’s generalization capabilities.

From the perspective of the data, a biased test set could significantly degrade the generalizability of the adaptation model (Liang et al. 2020). Derived from class-wise re-weighting (Cui et al. 2019), Dynamic online re-weighting (DOT) in DELTA (Zhao et al. 2023a) offers a dynamic approach to handle fluctuating and previously unknown class frequencies. Instead of directly determining class frequencies, DOT uses a momentum-updated class-frequency vector. Initialized with equal weights, the vector is updated at every inference step based on the current sample’s pseudo-label and existing weight. A significant weight (or frequency) for a particular class prompts DOT to diminish its contribution during subsequent adaptations. This methodology is pivotal in countering biased optimizations that might arise from inherent model training processes or even from situations like high inter-class similarities, thus maximizing the model’s generalizability.

Conjugate to Source: Previous OTTA methods, e.g., Tent, focus on entropy minimization to allow the adoption of the model with the absence of the test label. This naturally raises the question: What makes soft entropy a preferred choice? Conjugate PL (Goyal et al. 2022) has been proposed to shed light on this subject. To unearth the underlying mechanisms of the loss function, It begins by designing a meta-network to parameterize it. Observations indicate that the meta-output might echo the temperature-scaled softmax output of a given model. They further prove by conjugate adaptation loss that if the cross-entropy loss is applied in the source model, the soft entropy loss could represent the most proper loss during adaptation. This finding resonates with decisions made by Tent.

Feature representation learning: During adaptation in OTTA, there is no data label available. Therefore, the objective can be considered as a self-supervised learning task. AdaContrast is based on the concept of contrastive learning, which leverages positive pairs (different views of the same image) and negative pairs (features from different images). The idea is to bring positive pairs closer while pushing negative pairs away. Furthermore, AdaContrast modifies the InfoNCE loss (He et al. 2020) with the help of a memory queue to prevent samples from the same class from being pushed away.

In OTTA models, the choice of an optimization objective holds significant importance. It is evident that there is a prevailing trend toward the development of increasingly complex loss functions, as indicated by the growing number of baseline works. However, it is worth highlighting that the landscape of loss functions with superior adaptability and insensitivity to architectural variations remains somewhat limited, often characterized by their simplicity in terms of logical structure. These select loss functions, such as soft entropy, play a valuable role when constructing more intricate loss functions tailored to complex application scenarios.

3.1.4 Pseudo-labeling

As the mainstream of self-training, pseudo-labeling shows its significance in domain adaptation or semi-supervised learning tasks. However, things turn harder in OTTA due to the absence of the whole source set.

While only the test data is available during the current batch, **batch-level PL** emerges as a pragmatic approach. In alignment with standard **BatchNorm** optimization frameworks, **MuSLA** (Kingetsu et al. 2022) employs pseudo-labeling as post-optimization of the current batch to refine the decision boundary. While promising, this strategy introduces computational overhead, necessitating the processing of data batches multiple times, thereby prolonging adaptation phases and imposing increased memory requirements. Besides, the commonly used pseudo-labelling strategy in the teacher-student framework (e.g., **CoTTA** (Wang et al. 2022a), **RoTTA** (Yuan et al. 2023a)) identifies the student outputs of weakly augmented views as soft pseudo-labels. This could bring a stable optimization process during adaptation. Another category assumes the source pre-trained model has discriminability for confident test samples. Therefore, a threshold with pseudo-labeling for every single batch of data could be applied (Kingetsu et al. 2022).

Reliable PL. In obtaining reliable pseudo-labeling, a noteworthy challenge is the continuous data streams without the opportunity for review. Furthermore, the

covariate shift introduced between the source and test set could significantly degrade pseudo-labeling reliability. Under these circumstances, the establishment of a dependable pseudo-label becomes paramount. An avenue to address this challenge is presented by **TAST**, as introduced in (Jang et al. 2023). Unlike conventional thresholding methods that rely on the output of the current updated model, **TAST** adopts a prototype-based pseudo-labeling strategy. This approach derives pseudo-labels through the cosine distance between the model’s predictions and prototype representations. Importantly, these prototypes are constructed based on confident support samples in proximity, rendering them trustworthy compared to predefined thresholding approaches based solely on the linear layer output. This enhances pseudo-labels’ reliability in the face of dynamic model updates during online test-time adaptation. A similar idea is **AdaContrast** (Chen et al. 2022b), which borrows the idea from (Mitchell and Schaefer 2001). It proposes soft K nearest neighbors voting in the feature space to generate significantly more correct pseudo labels for each target sample.

To obtain a reliable pseudo-label, another idea is to utilize multiple augmentations. For example, majority voting (Wu et al. 2021) could directly bring reliable pseudo-labels with multi-augmentation assistance.

Complementary PL. Yet, as the discourse extends, an underlying challenge surfaces: one-hot pseudo-labels that focus singularly on the class with maximal confidence often incur significant information losses, particularly under the domain shifts. An alternative, **ECL** (Han et al. 2023), promotes a nuanced stance. This method doesn’t merely rely on maximum predictions for pseudo-labeling but factors in predictions beneath a set confidence threshold, thus introducing complementary labels to which the prediction does not belong. This intricate approach aspires to diminish the pitfalls linked with negative learning (Kim et al. 2019).

Discussion. In summary, the challenges associated with pseudo-labeling extend beyond label selection criteria and encompass broader considerations, including environmental constraints and operational efficiency. While pseudo-labeling shows promise in specific contexts like domain adaptation and offline test-time adaptation, its suitability diminishes in real-time prediction tasks. This highlights the need for further research and innovative solutions to address these operational challenges effectively.

3.1.5 Other Approaches

OTTA methods are developed for adapting models to new scenarios, but applying them in uncertain real-world situations requires careful consideration.

Venturing from the conventional path of adapting pre-trained model parameters, LAME (Boudiaf et al. 2022) presents an innovative approach. Instead of updating the model, LAME focuses on refining the model’s output. This is achieved by identifying latent assignments that maximize the manifold-regularized likelihood of the dataset. In a bid to further refine the output, Laplacian regularization is incorporated into the framework. Subsequently, a concave-convex procedure (CCCP) is formulated, augmenting the overall optimization process.

3.1.6 Summary

The optimization-based approach represents the most comprehensive category within online test-time adaptation. This category is underpinned by the fundamental notion that every machine learning model necessitates optimization, making it a universally applicable concept transcending architectural specifics. In the context of OTTA, the adaptation model’s optimization primarily revolves around attaining optimization consistency, stability, and robustness. However, it is crucial to highlight that the effectiveness of optimization hinges on data availability. Given that test data can only be adapted at the batch level, whether the model can be optimized to encapsulate the characteristics of the global test set remains an unaddressed aspect. To this end, the subsequent section will delve into data-driven methodologies, elucidating how data can play a pivotal role in OTTA.

3.2 Data-based OTTA

Data-based OTTA is motivated by the intricacies introduced by streaming data. While there’s a prevailing notion of fine-tuning models, it has become evident that mere optimization may not sufficiently address the complexities of diverse test datasets due to their batch-level updates. With the limited number of samples in each batch, encountering test samples with unexpected changes is inevitable. Recognizing the **pivotal role of data** for a reliable test data prediction could potentially fill this gap:

- Enhancing the model’s generalizability.
- Tailoring the model’s discriminative capacity to the current data batch.

While the broader landscape of OTTA methodologies encompasses a multitude of solutions, this section focuses specifically on data-centric strategies within OTTA approaches, highlighting the indispensable role of data by either diversifying the batch data (Sec 3.2.1) or preserving high-quality global-level data information (Sec 3.2.2) during test-time adaptation.

3.2.1 Data Augmentation

Data augmentation is crucial in domain adaptation (Wang and Deng 2018) and generalization (Zhou et al. 2023), primarily amplifying model transferability and generalizability. These traits are indispensable for test-time adaptation, especially when dealing with online test data.

Random Augmentation Strategies

Predefined augmentations. Prevailing data augmentation techniques such as cropping, blurring, and flipping are seamlessly integrated into certain OTTA methodologies, demonstrating their capacity to emulate specific data shifts. Aiming to obtain reliable predictions, a paradigmatic instance of this integration can be observed in OTTA techniques rooted in the mean-teacher model framework. These methods employ a weak-strong augmentation consistency approach. In ensuring prediction consistency across augmented views, these models facilitate extracting a generalized sample representation within the current batch. Notably, while PAD and TTPR (Sivaprasad et al. 2021) do not strictly adhere to the mean-teacher framework, both of them using common augmentation strategies (32 and 2 augmentations correspondingly) to support a consistent prediction, which bolsters model’s generalizability while maintains its discriminability. A distinct approach is delineated in MEMO, employing a comprehensive augmentation strategy, AugMix (Hendrycks et al. 2020), for every test image. For each individual data point, an array (typically encompassing 32 or 64) of augmentations from the AugMix set \mathcal{A} are produced to cultivate a resilient model.

Selective Augmentations. In the previous section, OTTA approaches often predetermine augmentation policies without addressing potential distribution shifts during inference. Given that test distributions can undergo substantial variations in continuously evolving environments, there exists a risk that such fixed augmentation policies may become ineffectual. In CoTTA (Wang et al. 2022a), rather than augmenting every test sample by a fixed strategy, augmentations are judiciously applied only when pronounced domain differences are detected, mitigating the risk of accumulating errors. PETAL (Brahma and Rai 2023) follows the idea of CoTTA

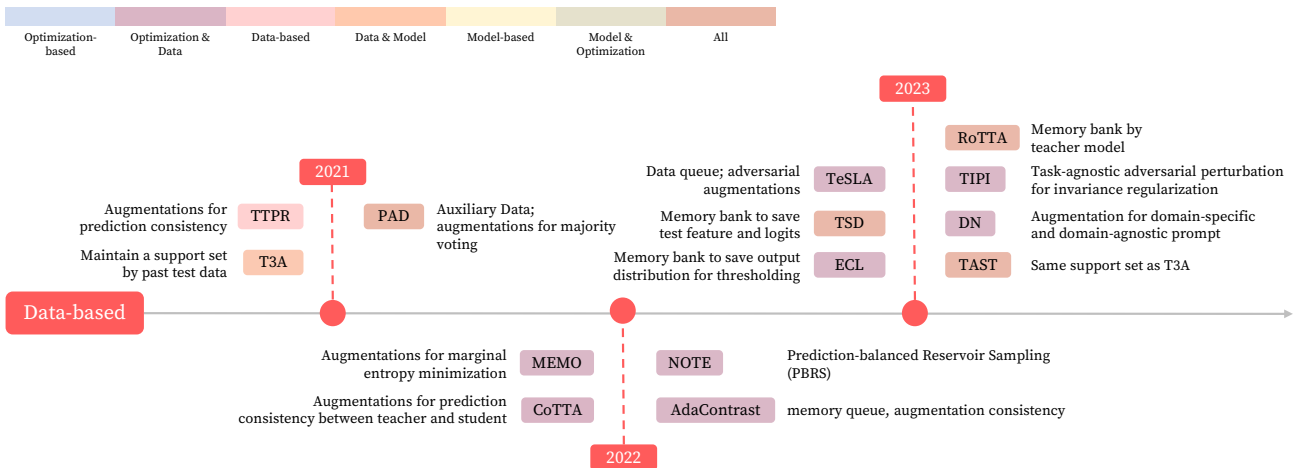


Fig. 6: Timeline of Data-based OTTA methods.

and applies augmentations to test samples for teacher input only if the domain difference is substantial.

Adversarial Augmentation

Traditional augmentation methodologies offer partial remedies but often fall short due to intra-domain disparities in test data, such as distribution variations and the data’s intrinsic learning value. TeSLA, as referenced by (Tomar et al. 2023), diverges from relying on pre-determined or randomly chosen augmentations. Instead, it capitalizes on adversarial data augmentation to ascertain the optimal augmentation strategy. This approach establishes a policy search space \mathcal{O} , comprising a gamut of augmentation strategies, each associated with a specific magnitude parameter, denoted as m . TeSLA then introduces a sub-policy, ρ , constituted of a pre-determined number of augmentations paired with their pertinent magnitudes. The teacher model then undergoes entropy maximization loss to assimilate the policy ρ . The underlying rationale is that entropy maximization discerns the augmentation policy that exhibits the most pronounced discrepancy in teacher model predictions. Refining the model with such pronounced perturbations facilitates an enhanced comprehension of the consistency inherent to individual test data.

3.2.2 Memory Bank

Surpassing the utilization of random, selective, or adversarial augmentations to diversify test data within the current batch, a memory bank emerges as an efficacious mechanism to select representative samples and preserve them for memory replay. This strategy can maintain the global statistics of the test data without imposing additional computational burden on OTTA.

The establishment of a memory bank entails addressing two fundamental considerations:

- **Selection Criteria for the Memory Bank:** Deciding what should be stored in the memory bank is the first crucial factor. This involves identifying which instances should be preserved for potential replay during testing.
- **Memory Bank Management:** The second factor pertains to how to maintain the memory bank. Specifically, it raises questions about the design of strategies for inserting new instances into the memory bank and deleting existing ones. These decisions are guided by considerations of effectiveness and necessity.

Considering these factors, memory bank strategies can be classified into two discrete categories: the time-uniform memory bank and the class-balanced memory bank. It’s worth noting that numerous approaches opt to include both types simultaneously.

In addressing the challenges posed by both temporally correlated distributions and class-imbalanced issues, NOTE (Gong et al. 2022) introduces the Prediction-Balanced Reservoir Sampling (PBRS) to save sample-prediction pairs. The ingenuity of PBRS lies in its fusion of two distinct sampling strategies: time-uniform and prediction-uniform. The time-uniform approach, reservoir sampling (RS), aims to obtain uniform data over a temporal stream. To be detailed, for a sample x being predicted as class k , we randomly sample a value p from a uniform distribution $[0, 1]$. Then, if p is smaller than the proportion of class k in whole memory bank samples, pick one randomly from the same class and replace it with the new one x . At the same time, the prediction-uniform part prioritizes the predicted labels to ascertain

the majority class within the memory. Upon identification, it supplants a randomly selected instance from the majority class with a fresh data sample, thereby ensuring a balanced representation. The design of PBRS ensures a more harmonized distribution of samples across both time and class dimensions, fortifying the model’s adaptation capabilities.

Similarly, RoTTA, introduced by (Yuan et al. 2023a), offers a Category-balanced sampling with timeliness and uncertainty (CSTU) module, dealing with the shifted label distribution. In CSTU, the author proposes a category-balanced memory bank M with a capacity of N , considering the timeliness and uncertainty of samples when updating. Data samples x in CSTU are stored alongside their predicted labels \hat{y} , a heuristic score \mathcal{H} , and uncertainty metrics \mathcal{U} . The heuristic score is calculated by:

$$\mathcal{H} = \lambda_t \frac{1}{1 + \exp(-\mathcal{A}/\mathcal{N})} + \lambda_u \frac{\mathcal{U}}{\log \mathcal{C}} \quad (10)$$

where λ_t and λ_u is the tradeoff between time and uncertainty, \mathcal{A} is the age (i.e., how many iterations this sample has been stored in the memory bank) of a sample stored in the memory bank. \mathcal{C} is the number of classes, \mathcal{N} is the capacity of the memory bank, and \mathcal{U} is the uncertainty measurement, which is implemented as the entropy of the sample prediction. This heuristic score \mathcal{H} is then used to decide whether a test sample should be saved into the memory bank for each class. As the lower heuristic score is always preferred, its intuition is that CSTU aims to maintain fresh (i.e., lower age \mathcal{A}), balanced, and certain (i.e., lower \mathcal{U}) test samples. thereby enhancing adaptability during online operations.

Considering class-balanced data preservation, TeSLA (Tomar et al. 2023) introduces a fixed-size online queue. The underlying concept involves the preservation of pairs comprising weakly augmented refined sample features and their corresponding pseudo-labels. This preservation is conducted considering their predicted class assignments and adheres to the principle of first-in, first-out. Subsequently, these preserved pairs enhance pseudo-label predictions through interactions with their nearest neighbors within the queue.

TSD (Wang et al. 2023) distinguishes itself as an outlier among memory bank-based methodologies, as it does not neatly fit into any existing category. Its objective centers on preserving complete information of test samples, to suit the online setting. In the context of TSD, as new test samples are encountered, the sample’s embedding and associated logit will be saved in a memory bank. These stored representations are subsequently utilized for prototype-based classification. Notably, TSD adopts a strategy inspired by T3A (Iwasawa

and Matsuo 2021) to initialize its memory bank by the weights of the source pre-trained linear classifier.

An additional departure from the conventional approaches is found in the work by ECL (Han et al. 2023). ECL introduces a fixed-length memory bank to store output distributions. This memory bank serves as prior information for thresholding complementary labels, which, in turn, is utilized to refine the model’s updates. Subsequently, the memory bank undergoes a refreshment process facilitated by the updated model parameters.

AdaContrast also uses a memory queue to avoid push-away pairs from the same class in contrastive learning. The memory queue is designed for saving all previous key features with corresponding pseudo-labels.

3.2.3 Summary

Utilizing data-based techniques can prove advantageous in scenarios where a test set exhibits bias or is constrained by specific stylistic limitations. Nonetheless, this approach introduces an additional computational burden, which can be unanticipated in online settings. In the subsequent section, we will explore an alternative perspective, examining how architecture changes can yield benefits in OTTA.

3.3 Model-based OTTA

In contrast to data-centric OTTA, which emphasizes predictive consistency regularization amidst diversified or restored samples, model-centric OTTA approaches alter the model architecture to mitigate distribution shifts. Specifically, architectural modifications are generally classified into two predominant categories: i) the incorporation of novel branches, and ii) the substitution of selected layers. Recently, a novel paradigm of test-time prompting has been introduced, particularly tailored for transformer-based models, which adroitly learn a concise set of parameters to adeptly accommodate the emergent distribution.

3.3.1 Module Addition

Input Transformation. Unlike the commonly used optimization methods, SLR (Mumjadi et al. 2021) introduces an input transformation module (i.e., $g = f \circ d$, where f is the source model) to cancel the test-time distribution shifts partially. This configuration pre-appends a trainable network, d , to the source model f , enhancing its capacity to mitigate domain shifts. The transformation function, $d(x)$, is designed as a convex combination of the original input and a transformed variant,

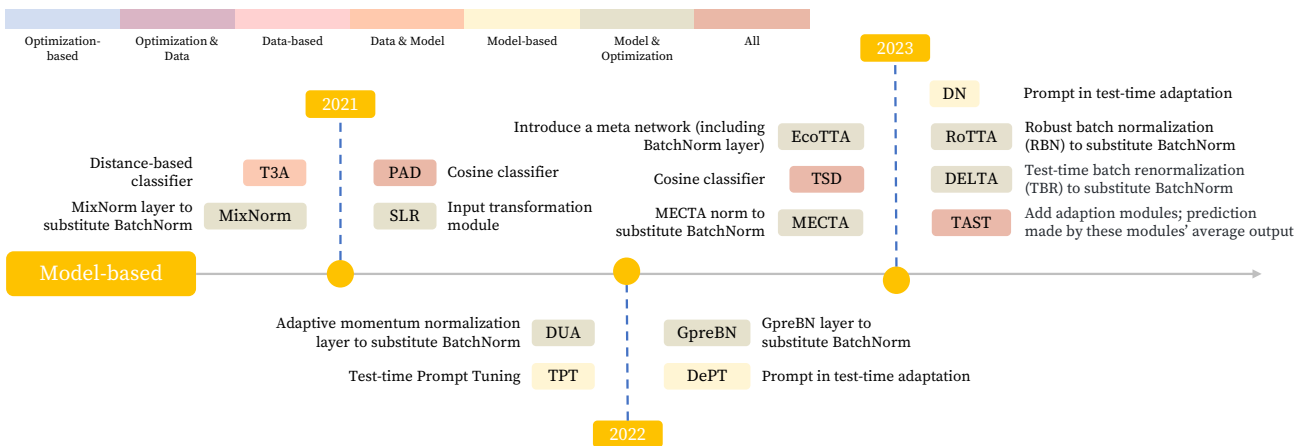


Fig. 7: Timeline of Model-based OTTA methods.

ensuring both versatility and maintainability. Interestingly, at initialization, this ensures $d(x) = x$ and $g = f$, providing a stable starting point. Crucially, the design objective of d is to partially address domain discrepancies without relying on source domain samples during the full test-time adaptation phase. As the adaptation targets only a subset of parameters, the method retains the innate features of the pre-trained model, especially the convolutional kernels.

Adaptation Module. Rather than directly inserting a specific layer, TAST (Jang et al. 2023), incorporates a uniquely initialized adaptation module atop the feature extractor. The primary task of this module during test time is to train using prototype-based class distributions to predict labels for the test data. Despite the potential benefits, one intrinsic challenge is the potential performance degradation arising from the random initialization of the adaptation module. To navigate around this issue, ensemble strategies have been proposed, where the adaptation modules are trained individually. Specifically, **BatchEnsemble** (Wen et al. 2020) is applied as the adaptation module to benefit information exchange between modules. By amalgamating predictions from these independently trained modules, the objective is to achieve more accurate and robust label predictions, presenting a promising frontier for enhancing test-time adaptation performance.

Classifier. Cosine similarity-based classifiers (Chen et al. 2009) have emerged as a popular choice, notably outperforming traditional linear classifiers. By prioritizing the angle between vectors, cosine similarity ensures the accurate classification of data samples and delivers a deeper understanding of the inherent semantic relationships. Building on the robust foundation of cosine similarity-based classifiers, TAST (Jang et al. 2023) introduces a cosine distance-based classifier. By averaging

across all adaptation module predictions, TAST achieves a more reliable prediction.

Similarly, TSD (Wang et al. 2023) opts for a cosine similarity-based classifier, deriving predictions from the features of the current sample in conjunction with its K-nearest neighboring features in the memory bank. Similar to TAST and TSD, PAD (Wu et al. 2021) also employs a cosine similarity-based classifier. However, there’s a key difference in how each approach maintains its prototype information. While TAST and TSD necessitate the upkeep of a queue to save test data information, PAD takes a more streamlined approach to save source information. According to its illustration, the weights updated through backpropagation in the trained cosine classifier can naturally function as the prototypes for each source class. This eliminates the need for maintaining a separate set of class prototypes or features, offering a more efficient way to capture the essence of each class.

3.3.2 Module Substitution

Layer substitution typically refers to swapping out an existing layer for a new one. Yet, when viewed through the lens of updating **BatchNorm** statistics, any method related to **BatchNorm**—barring those straightforwardly optimized by a set loss—can be considered under this umbrella. Examples of this include MECTA norm (Hong et al. 2023), MixNorm (Hu et al. 2021), RBN (Yuan et al. 2023b), and GpreBN (Yang et al. 2022), etc. We won’t delve into these methods again in this section to prevent redundancy.

3.3.3 Prompt-based Method

Another new category to address test data drift is the so-called **test time prompt Tuning** originating from

CLIP (Radford et al. 2021). Its basic idea is instead of fine-tuning the vision representation (which may cause loss of model generalizability), it fine-tunes the prompting, which modifies the context of the model input and thus does not distort pre-trained features. One representative of time-time prompt tuning is TPT (Shu et al. 2022), which aims to promote the consistency of the model’s predictions across different test image augmentations. Specifically, for each test image, N randomly augmented views from an augmentation set are generated, and the prompting parameter is further updated by minimizing the entropy of the averaged prediction probability distribution across these augmented views. It is worth noting that a confidence selection strategy is proposed to filter out the output with high entropy to avoid noisy updating brought by augmentations.

The usage of prompts could also benefit test-time adaptation performance. A prime instance is “Decorate the Newcomers” (DN) (Gan et al. 2023), Rooted in prompt learning, DN leverages the mean-teacher model in conjunction with the frozen source pre-trained model to acquire domain-specific and domain-agnostic prompts. It adheres to the same framework as the mean-teacher model to elucidate, receiving weak and strong augmented images as input. To decouple the invariance and specifics of the test image, DN employs two distinct loss functions. Domain-specific information is acquired through the cross-entropy loss between teacher and student model outputs. Furthermore, a parameter insensitivity loss is introduced to penalize parameters susceptible to domain shifts. This, in turn, ensures that the updated domain-insensitive parameters can effectively consolidate domain-agnostic knowledge. The learned prompt is appended to the test image during testing, and predictions are finally obtained from the frozen source model.

Except for designing a new module for learning the prompt, DePT (Gao et al. 2022) proposes to prepend prompts into the transformer architecture for test-time adaptation. The transformer model is first split into multiple stages. Then, for each stage, a learnable prompt is added, which makes the prompt learning natural to be a pure test-time adaptation task. During adaptation, only learnable prompts and the classifier is updated. Similar to DN, DePT applies a mean-teacher model with weak-strong augmentations, with the difference that the student model will allow both weak and strong augmentations. With the help of a preserved memory bank, a cross-entropy loss is applied between the memory bank-guided pseudo label and the output of the strong augmented test sample from the student model. The DINO (Caron et al. 2021) loss with prompt regularization is then added to the final objective to fine-tune the prompt.

3.3.4 Summary

While model-based OTTA methods exhibit effectiveness, their prevalence is overshadowed by the former two groups, primarily due to their inherent dependence on specific backbone architectures. Notably, during layer substitution and addition, even incremental modifications can yield substantial improvements in test-time performance, often obviating the need for alterations in original training paradigms. Such adaptability mechanisms, reminiscent of the “hot-swapping” concept, offer a novel viewpoint for tackling diverse data distributions. A cornerstone of the model-based paradigm is its synergistic relationship with prompting, a strategy empirically validated for enabling zero-shot inference. This synergy affords the model an ability to adapt to test instances in a coherent and reliable fashion, positioning it as a promising route for augmenting adaptability and trustworthiness in OTTA contexts.

4 Empirical Study

In this empirical study, we will focus on upgrading existing OTTA methods to accommodate the ViT model from the new era. Our primary objective is to investigate the transferability of the proposed idea that could be migrated to transformers. Additionally, we will provide solutions for substituting the existing components.

In order to comprehensively evaluate the performance of OTTA methods, we conducted a rigorous assessment of seven well-established OTTA algorithms. To ensure fairness and impartiality, we followed a standardized testing protocol. We selected a diverse set of datasets, including four artificial and two real-world shifted data sets. The CIFAR warehouse dataset repository played a central role in our evaluation, offering a wide range of subset, including real-world variations sourced from different search engines and images generated through diffusion-based processes. Specifically, we focused on two subsets of the CIFAR warehouse dataset in our survey: the Google image subset and the Diffusion image subset. These subsets were chosen to facilitate simulations of both real-world and artificial data shifts, allowing for a comprehensive assessment of OTTA methods.

4.1 Implementation Details

Optimization Details. In our experimental setup, we employed the PyTorch framework for implementation. The foundational architecture for all approaches is ViT base patch 16 ($224 * 224$) (Dosovitskiy et al. 2021),

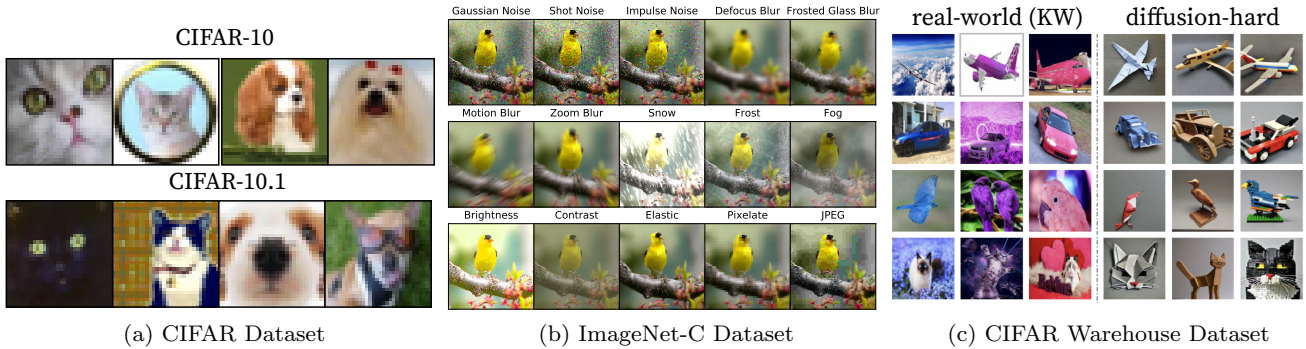


Fig. 8: The exemplars of the adopted datasets. The dataset shift includes variations in colors, synthetics data and types of corruptions.

serving as the network backbone. This backbone architecture is sourced from the Timm repository ¹. Our training regimen for the source model on the CIFAR-10 dataset comprised 8,000 iterations, including a warm-up phase spanning 1,600 iterations. The training was conducted with a batch size of 64, employing the Stochastic Gradient Descent (SGD) optimization algorithm with a learning rate of 0.03. For the CIFAR-100 dataset, we retained an identical configuration, with an extended training duration of 16,000 iterations and a warm-up period spanning 4,000 iterations. The source model for the ImageNet-1k dataset ² was directly acquired from the Timm repository. Additionally, we applied basic data augmentation techniques, namely random resizing and cropping to 224 pixels, consistently across all methods. To ensure consistency in the adaptation approach, specific settings are uniformly applied. The Adam optimizer with a momentum term β of 0.9 and a learning rate of $1e-3$ is employed to optimize the model. For all datasets, resizing and cropping techniques are applied as a default preprocessing step. During testing, a uniform normalization setting of (0.5, 0.5, 0.5) is adopted to mitigate potential performance fluctuations that may arise from external factors beyond the algorithm’s core operations.

Component substitution. To facilitate the adaptation of core methods for application on the Vision Transformer (ViT), we have devised a set of fundamental strategies:

- **Transition to LayerNorm:** In light of the absence of a Batch Normalization (BatchNorm) layer in ViT,

¹ <https://github.com/huggingface/pytorch-image-models>

² `vit_base_patch16_224.orig_in21k_ft_in1k` from https://github.com/rwightman/pytorch-image-models/releases/download/v0.1-vitjx/jx_vit_base_p16_224-80ecf9dd.pth

one key approach involves substituting all BatchNorm updates with LayerNorm updates.

- **Mixup Factors Adjustment:** It is imperative to eliminate any mixup factors applied to original methods based on BatchNorm, as LayerNorm does not consider statistics derived from other data samples.
- **Exclusion of Source Statistics:** Given that LayerNorm does not maintain running statistics, we exclude any components responsible for updating statistics related to the source data.
- **Feature Representation Adjustment:** In scenarios where feature representation is a prerequisite in the OTTA methods, a viable alternative is to replace it with the class embedding (i.e., the first dimension of the feature representation from ViT feature extractor), as this feature constitutes the foundation upon which final predictions are predicated.
- **Pruning of Incompatible Components:** Lastly, it is imperative to disregard any components that cannot be effectively implemented on the ViT backbone, ensuring compatibility with the model’s architecture.

These strategies serve as the groundwork for enabling the seamless integration of core methods with ViT, thereby extending the applicability of these methods to the Vision Transformer framework.

Baselines: To systematically assess and investigate the adaptability of OTTA methods to new backbone architectures, we have judiciously curated a set of seven general and versatile methods for our study. These methods include:

1. **Tent:** A classic OTTA method rooted in BatchNorm updates. To reproduce it on ViTs, we have replaced its BatchNorm updates with a LayerNorm updating

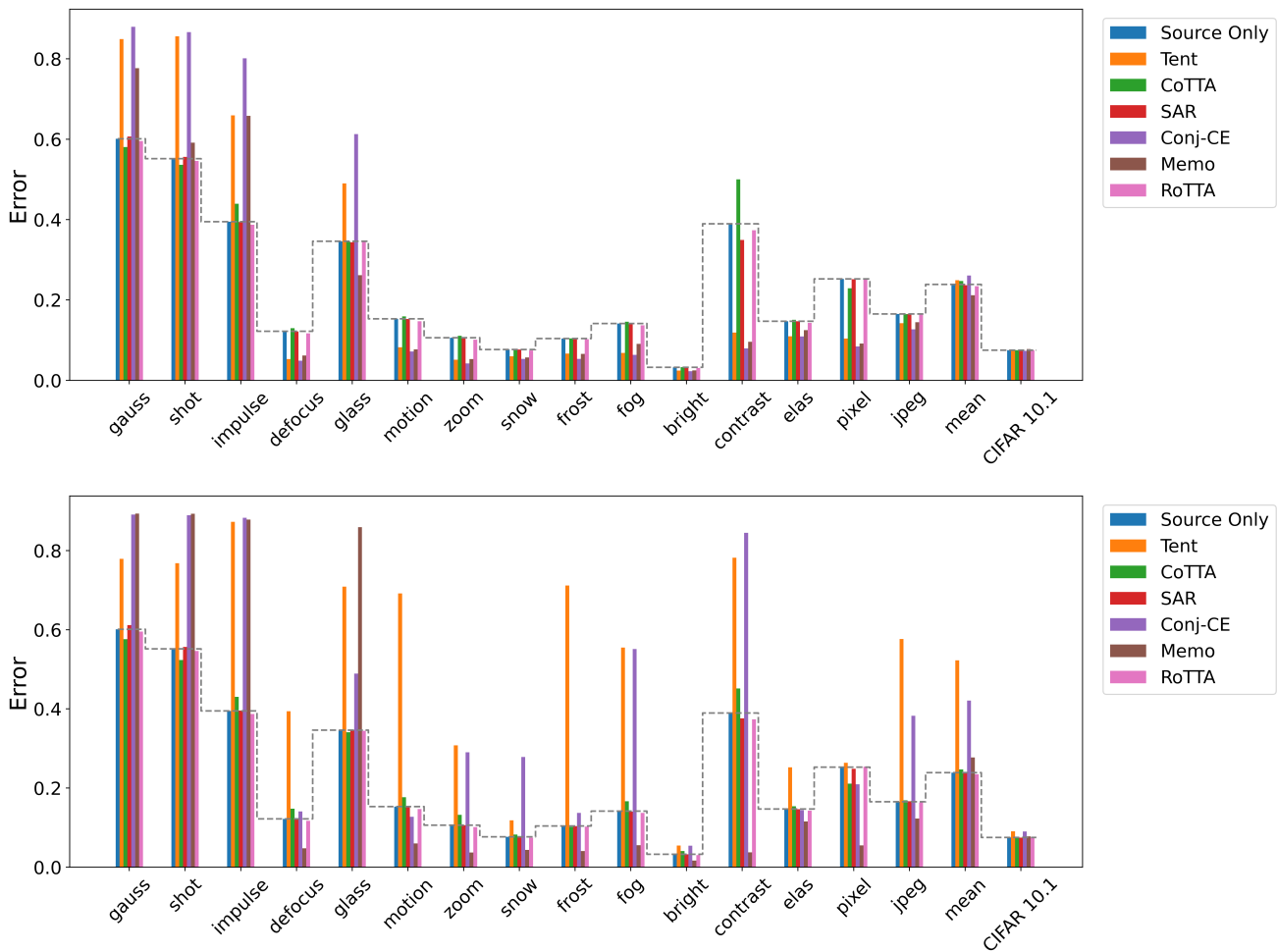


Fig. 9: Comparison of the OTTA performance on the CIFAR-10-C and CIFAR-10.1. The upper/bottom plots show the experiments conducted with batch size 16 / 1 based on the LayerNorm updating strategy, respectively

strategy, utilizing soft entropy as the optimization objective.

2. **CoTTA**: A representative approach that employs the mean-teacher model, parameter reset, and selective augmentation strategy. While it typically necessitates updating the entire student network, we have further assessed the LayerNorm updating strategy on the student model in our experimental design. Additionally, we have deconstructed CoTTA based on its parameter reset strategy, resulting in four variants: (1) Parameter reset with LayerNorm updating, (2) Parameter reset with full parameter updating, (3) Updating LayerNorm without parameter reset, and (4) Full network updating without parameter reset.
3. **SAR**: This method utilizes Sharpness-aware Minimization (SAM) to seek flat minima, employing the soft entropy loss. We investigate its effectiveness on the ViT model, incorporating the defined Adam optimizer.

4. **Conjugate PL**: As we train the source model by cross-entropy loss, it is similar to Tent but with the distinction of allowing the model to interact with the data twice: once for updating and once for prediction.
5. **MEMO**: Two versions of MEMO are considered for benchmarking OTTA on ViT: one with full model updating and another with LayerNorm updating. We have removed all data normalizations from its augmentation set to maintain consistency and prevent unexpected performance variations.
6. **RoTTA**: RoTTA encompasses ideas from all three OTTA categories. During our experiments, we exclude its RBN module, as LayerNorm in ViT is designed to handle data at the sample level, rendering the RBN module inapplicable.
7. **TAST**: TAST spans three OTTA categories and necessitates feature representation for distance-based classification. In our evaluation, we employ the class

embedding in the first dimension as the samples' feature representation, aligning with ViT's use of the classifier's input.

Despite the many available OTTA methods, thoroughly evaluating this selected subset will yield valuable insights commensurate with our expectations. In this survey, we answer the following research questions:

4.2 Is OTTA still working with ViT?

For an assessment of the chosen OTTA methods' efficacy, we compare them against the source-only baseline, which denotes inference devoid of adaptation. We address this question individually for each dataset in the subsequent sections.

4.2.1 On CIFAR-10-C and CIFAR-10.1 Benchmarks

As illustrated in Fig. 9, We fully evaluate the CIFAR10-C and CIFAR-10.1 datasets, with batch sizes 1 and 16, to simulate the streaming data and limited computational environment. To clearly understand the pattern of predictions, we categorize our observations into three aspects: 1) variation in types of corruption, 2) variation in batch sizes, and 3) variation in adaptation strategies.

- **Noise-based corruptions.** As depicted in Fig. 16, we observe a significant issue with noise corruptions where most methods, including direct inference, experience high error rates regardless of their batch size. This could be attributed to the substantial domain shift that most methods are unable to handle. Adapting to noise corruption is a challenging task for entropy-based methods and MEMO, regardless of their batch size. This could be attributed to the significant domain gap discussed earlier. While uncertainty based optimization aims at increasing the model's confidence, it is unable to correct wrong predictions directly. MEMO also relies on predictions to a certain extent, and therefore, exhibits similar patterns. It is observed that consistent results are obtained irrespective of the batch size in the defocus blur (defocus), pixelate (pixel), and brightness (bright) domains. This may be due to the slight domain gap between these two corruptions and the source image. However, it is noted that the performance of Tent is significantly inferior to the baseline direct inference, which is consistent with other domains when the batch size is 1.
- **Batch size.** Changes in the batch size will not change too much in terms of the mean error, except for those soft entropy-based methods. This could

refer to Sec. 4.4, where a large batch size could stabilize the optimization process. Similar observation could be found in CIFAR10.1, where two soft entropy-based methods (Tent and Conj-CE) fail at small batch sizes.

- **Adaptation strategy.** SAR and RoTTA perform stable regardless of the domains and batch size. RoTTA is insensitive to batch size as it maintains a memory bank to save fresh and reliable data. This additional high-quality data information can mitigate the performance degradation of small batch sizes. On the other hand, SAR aims to achieve flat minima, ensuring that the model is optimized for stability preventing biased learning during adaptation. MEMO performs well on certain domains, even when the batch size is as small as 1. This is a deliberate feature of MEMO, which was designed to support extremely small batch sizes. However, the difference in performance between various domains using MEMO highlights that some marginal distributions are difficult to estimate accurately or are flawed, resulting in significant disparities among domains.

4.2.2 On CIFAR-100-C Benchmark

The pattern of errors in CIFAR-100-C is similar to that of CIFAR-10-C. However, the performance of OTTA methods is worse when the batch size is set to 16. To avoid redundancy, we only discuss the different patterns observed in CIFAR-100-C.

- CoTTA performs worse for some corruption domains when the batch size is set to 16. This could be due to the fact that as the number of classes increases (from 10 to 100), the adaptation becomes harder. Additionally, the parameter reset strategy aims to select a fixed ratio of model parameters and reset them to the source pre-trained one, leading to an unlearning process. In simpler terms, this means that the model has not learned much knowledge on the new domains and its existing knowledge has already been partially deleted.
- In certain domains, SAR begins to exhibit limitations, particularly in the presence of noise distortions such as Gaussian noise, shot noise, and impulse noise. One possible explanation for this is that, rather than seeking a flat minimum by a constant ratio as in SAM, the optimization of CIFAR100C may not align in the correct direction.
- Regardless of the batch size, the degradation of the contrast corruption domain worsens over time. As indicated in Figure 10, only RoTTA can consistently exceed direct inference in the contrast column. This

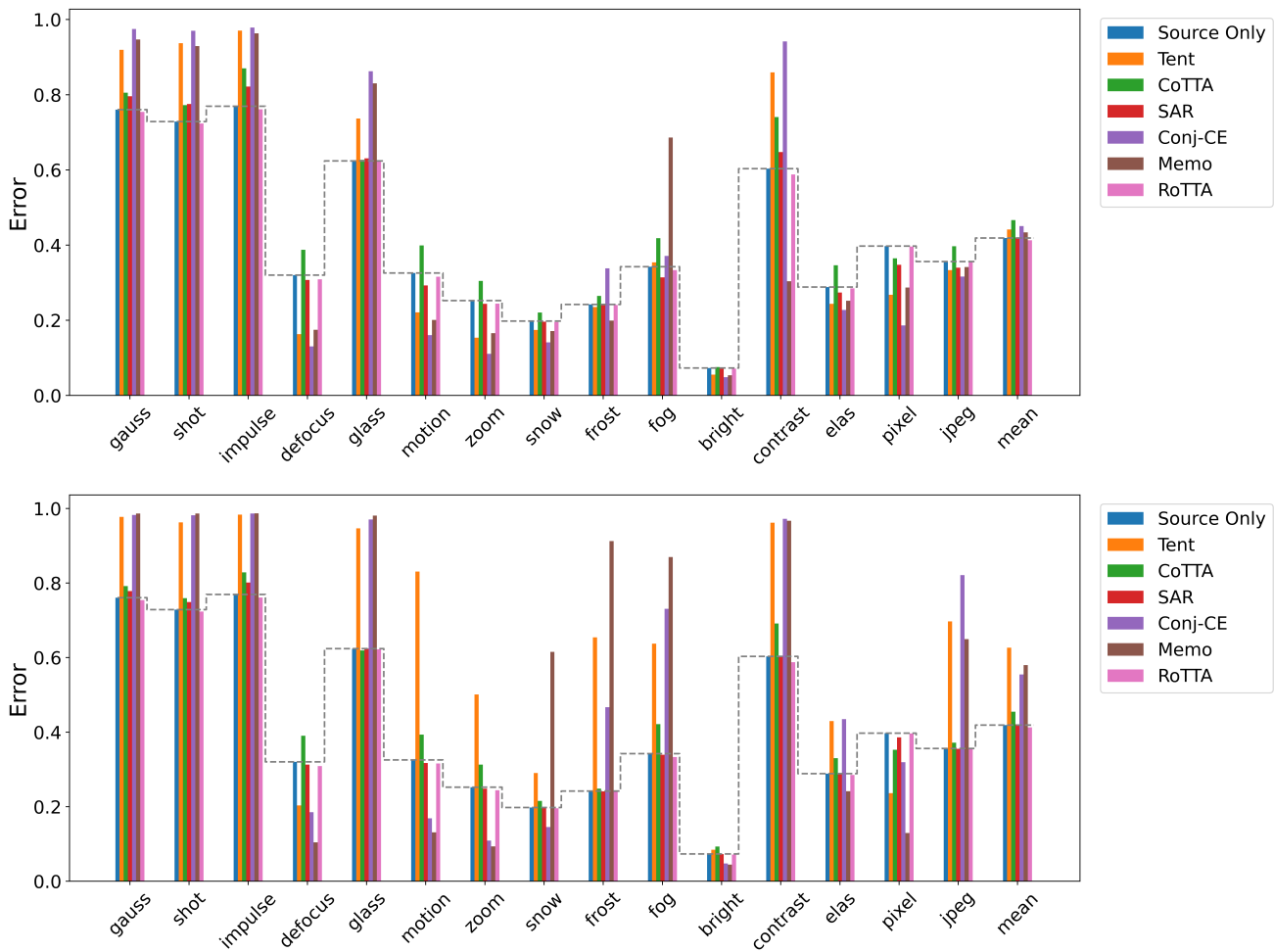


Fig. 10: Comparison of the OTTA performance on the CIFAR100C. The upper/bottom plots show the experiments conducted with batch size 16 / 1 based on the LayerNorm updating strategy, respectively

implies that preserving valuable sample information is crucial, particularly for challenging domains.

4.2.3 On Imagenet-C Benchmark

Compared with CIFAR10C and CIFAR100C, ImageNet-C shows more difference patterns. As illustrated in Figure 11, when the batch size is 16, only SAR, Conj-CE, and RoTTA perform better than the source model inference in terms of the mean error. On the other hand, Tent, MEMO, and CoTTA exhibit significantly poor results. The error rate within each domain follows a similar pattern. There could be several potential reasons for this. Firstly, there might be an intra-domain gap in the ImageNet dataset, which could be diverse within each class. This situation causes two gaps to exist simultaneously, thereby hindering the adaptation potential. Secondly, it is possible that the model is struggling to learn certain knowledge, which is similar to the

phenomenon described in Section 4.2.2. In this case, a parameter reset in CoTTA could further deteriorate the model’s discriminability.

In terms of batch size 1, only RoTTA survives. It emphasizes the importance of informative data saving, indicating that when facing severe shifts, some specific design is necessary.

4.2.4 On CIFAR-Warehouse

We assess OTTA techniques on the CIFAR-10-warehouse dataset, encapsulating real-world shifts across 10 classes consistent with CIFAR. For clarity, we choose two representative domains to highlight real-world shift and diffusion synthesis shift.

The **Google split** within the CIFAR-warehouse comprises images sourced from the Google search engine, serving as a testament to contemporary OTTA meth-

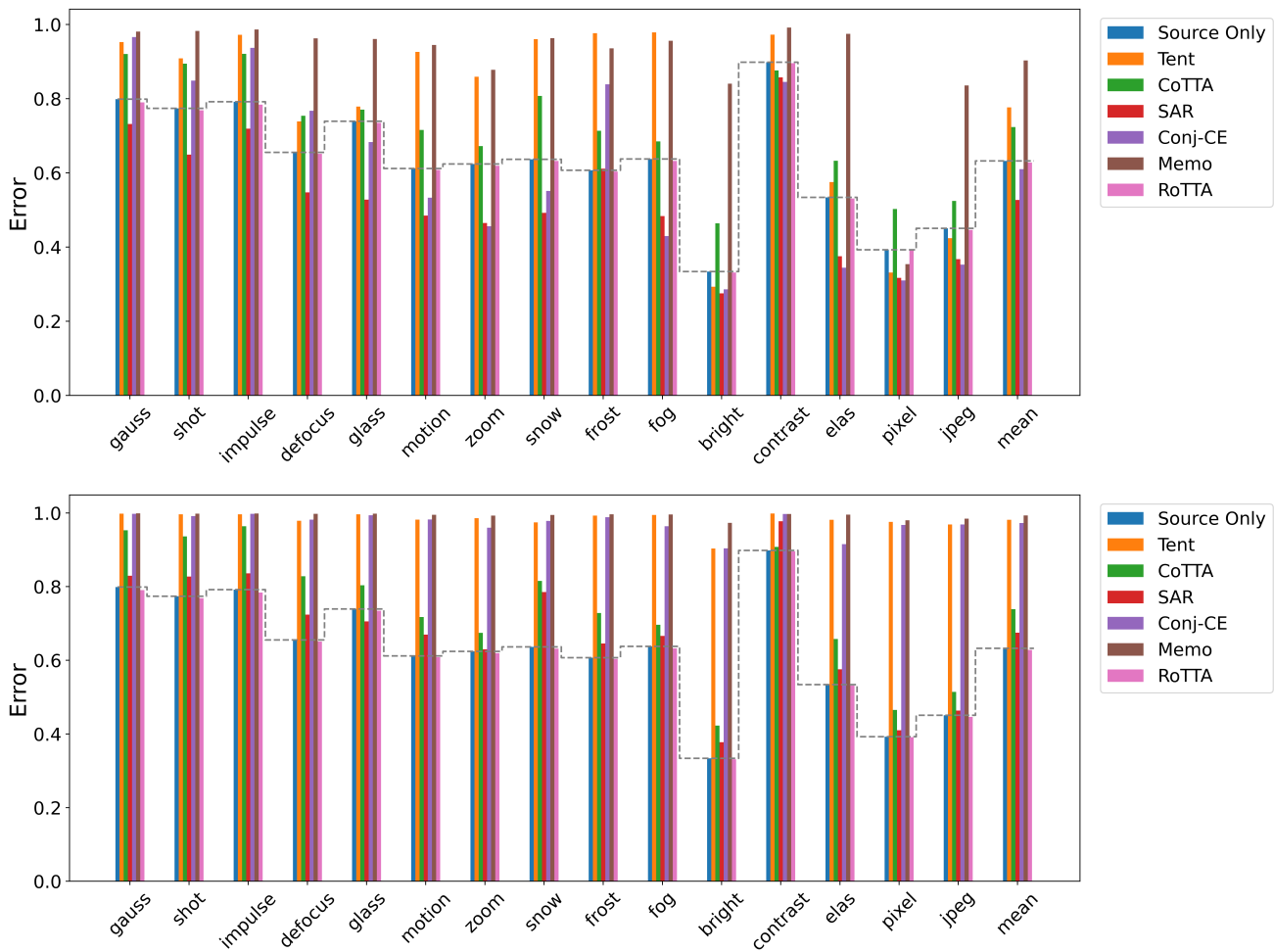


Fig. 11: Comparison of the OTTA performance on the ImageNet-C. The upper/bottom plots show the experiments conducted with batch size 16 / 1 based on the LayerNorm updating strategy, respectively

ods’ aptitude in managing real-world distributional deviations.

Based on the results presented in Figure 12, we have the following observations regarding the Google split.

- When the batch size is 16, most of the examined OTTA methods perform similarly or even better than direct inference. The top figure of Fig. 12 shows that the baseline performance (represented by the dotted line) has a higher error rate than the OTTA methods in most subdomains. This suggests that the existing OTTA methods are, at least, unlikely to deceive the source pre-trained model.
- In certain domains, uncertainty reduction techniques may not work as expected. Specifically, in domain G-09, most uncertainty-based methods tend to fail. This could be due to an unexpectedly large gap in those domains. However, other methods, such as RoTTA and SAR, still manage to perform well by

either preserving high-quality data information or seeking flat optimization to mitigate domain shift.

When the batch size is 1, the pattern is clearer, as shown in Fig. 12.

- Uncertainty-based methods cause performance degradation in nearly all domains, which may be due to instability with extremely small batches of data. This even becomes a must in **Tent**.
- RoTTA and SAR exhibit exceptional stability regardless of batch sizes, as observed in Sec. 4.2.1

Regardless of the batch size, there are some observations that can be made. Firstly, for G-07, all OTTA methods and direct inference perform similarly, irrespective of batch size. Interestingly, even when the batch size is just 1, most methods achieve better results than a batch size of 16. This is probably due to the fact that each test sample is informative enough but also diverse from one another. When mixed together, it confuses

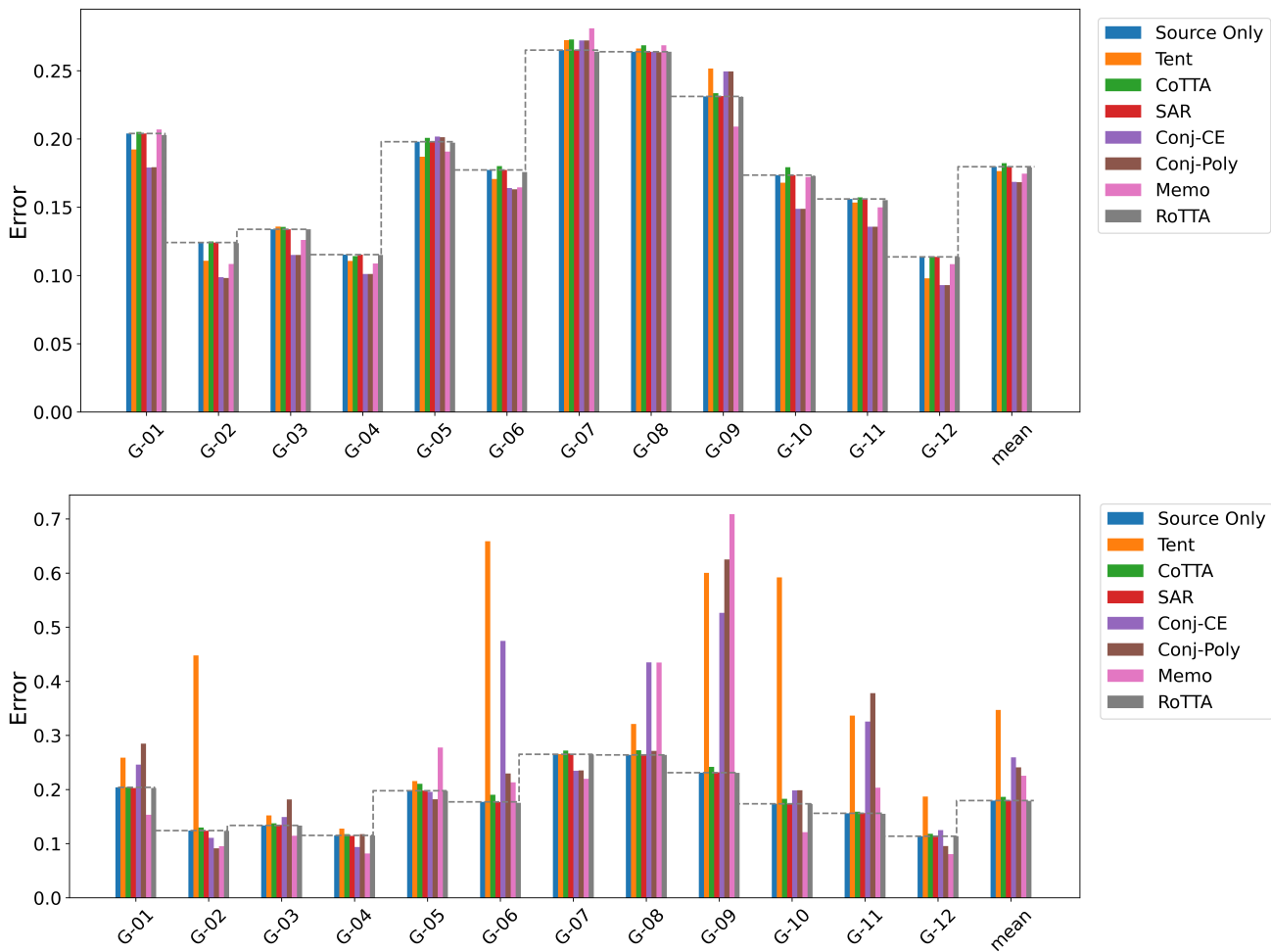


Fig. 12: Comparison of the OTTA performance on the **Google split** of CIFAR-10-Warehouse. The upper/bottom plots show the experiments conducted with batch size 16 / 1 based on the LayerNorm updating strategy, respectively

the model rather than stabilizing the adaptation, as the model doesn’t have a clear direction to follow.

Secondly, G-09 fails for most of the cases, regardless of batch size. Unlike the above observation, this is potentially because of the large domain gap, where rare methods could potentially mitigate it.

Diffusion split. We also evaluated OTTA methods within the diffusion domain of the CIFAR-warehouse dataset. The results, as depicted in Fig. 13, reveal a consistent pattern in the performance of all methods across 12 subdomains, except for domain DM-05.

- **Tent** and Conjugate PL methods, which follow the uncertainty reduction objective described in Section 3.1.3, show worse performance on DM-05 than pure inference. This anomaly can be attributed to a significant domain shift, resulting in a biased understanding of the information. The incorrect indica-

tor learning in the uncertainty-based loss function could further lead to model biases.

- On the contrary, these uncertainty-based algorithms show superior performance among other domains, further indicating the hard level for each diffusion-based subdomain.

Besides these intuitions, particularly noteworthy is the stable performance of CoTTA, SAR, and RoTTA. Firstly, since SAR borrows the idea from SAM, it is seeking a flat minimum. The model will be optimized to a data-insensitive area, which allows not only a certain prediction delivered by its soft entropy loss, but also, most importantly, stable predictions. With the parameter reset strategy, CoTTA could control the biased adapting, allowing the partial recovery of the knowledge from the source domain. This could be seen as an important factor in CoTTA’s stable performance, even in the DM-

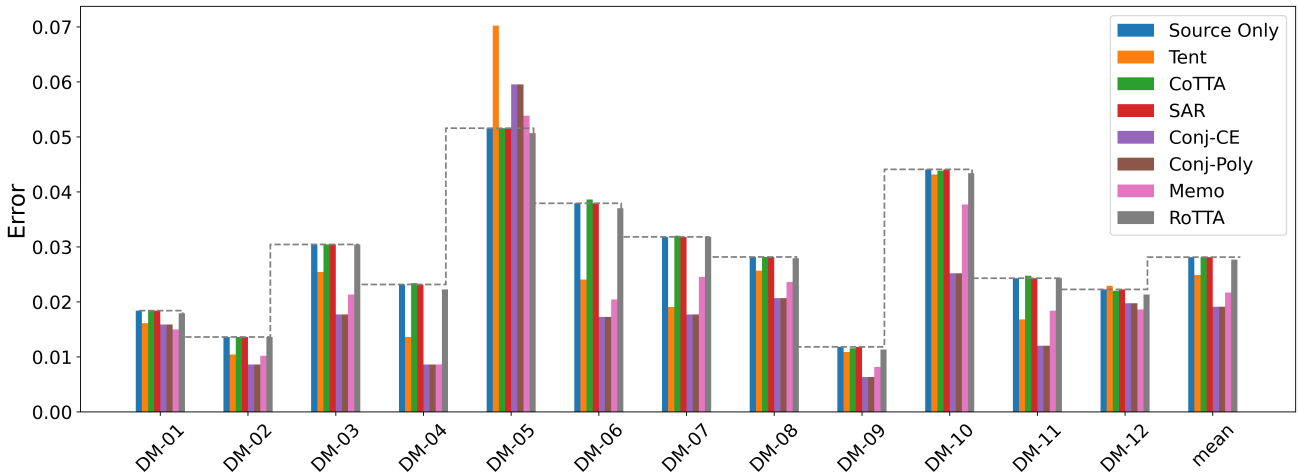


Fig. 13: Comparison of the OTTA performance on the **diffusion split** of CIFAR-10-Warehouse. All the experiments are conducted with batch size 16 based on the LayerNorm updating strategy. The dotted line indicates the baseline performance without any adaptation.

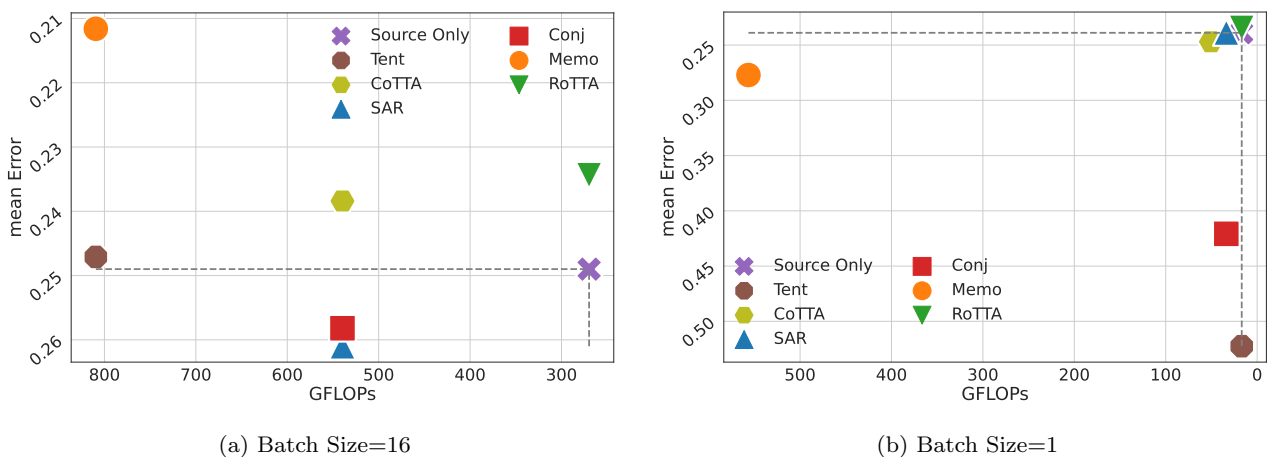


Fig. 14: Mean error vs Giga Floating Point Operations Per Second (GFLOPs). We plot the correlation between them under batch size 16/1 settings for the CIFAR-10-C dataset.

05 subdomain. **RoTTA**, by maintaining a well-designed memory bank, also achieves similar results as in **CoTTA**. These two algorithms could both be treated as a solution by maintaining useful information but different strategies.

Conclusion. Based on the experiments conducted, we discovered that most methods follow a similar pattern across different datasets. This demonstrates that the current OTTA method has the potential to tackle various covariate shifts. Notably, **RoTTA** and **SAR** consistently performed well and remained stable across different domains. This is particularly significant since we observed that different domain types could significantly impact the model adaptation process. The characteris-

tics exhibited by these two methods could potentially contribute to future research in this area.

4.3 Is OTTA efficient?

In order to evaluate the effectiveness of certain OTTA algorithms in practical applications, especially when there are hardware limitations, we propose using GFLOPs as the measure of efficiency. In Fig. 14, we can observe the relationship between the performance of OTTA models and their corresponding GFLOPs for batch size 1 and 16 cases. Our main objective is to investigate how the computational expense of a model is related to its performance.

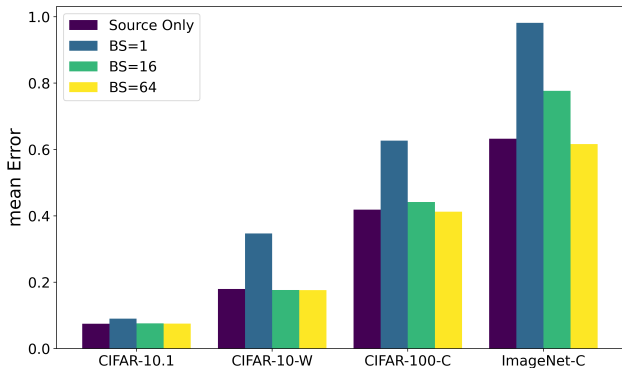


Fig. 15: Impact of varying batch sizes on CIFAR-10.1, CIFAR-10-W, CIFAR-100-C, ImageNet-C. The base model is **Tent** optimized on **LayerNorm**.

When it comes to evaluating performance, lower GFLOPs and mean error is always preferred. Based on this criterion, we have found that **MEMO** prioritizes high performance at the cost of computational efficiency. This is due to the BALD optimization strategy for the averaged marginal distribution employed by **MEMO**. However, some OTTA methods can balance the trade-off between these two evaluation metrics. Specifically, when the batch size is 16, **RoTTA** can achieve low error rates while also providing effective model updates.

As shown on the right-hand side of the figure, with a batch size of 1, most OTTA methods offer satisfactory performance while requiring a low computational cost. **RoTTA**, in particular, demonstrates superior hardware requirements and performance, even when compared to **Tent** with a batch size of 16. This first indicates that choosing a small batch size can help reduce the hardware requirements. However, it’s important to note that using an extremely small batch size, while beneficial for hardware capacity, may also reduce the accuracy of the model to some extent. This is particularly true when compared to a batch size of 16. Secondly, choosing a proper model can improve performance based on two evaluation metrics, regardless of batch size, but may not be the best when evaluating separately.

In conclusion, reducing the batch size is a straightforward and practical solution to manage the hardware capacity. However, it is important to keep in mind that this may impact the model’s accuracy. A careful balance should be struck between these two factors based on the particular deployment scenario.

4.4 Is OTTA sensitive to Hyperparameter Selection?

Batch Size still Matters!... but not too much. One un-neglectable factor in the OTTA setting is its batch size.

Since the data is coming and being processed at the batch level, performance sensitivity in terms of its batch size shows an important examination factor.

As shown in Fig. 16, we study the impact of varying batch sizes on **Tent**’s performance when used with the CIFAR-10-C dataset. The results indicate that the performance of **Tent** is heavily influenced by the batch size within the range of 1 to 16, for most corruptions. However, the correlation between the model’s performance and its batch size is significantly reduced for batch sizes 16, 32, 64, and 128, indicating less correlation between **LayerNorm** updating and batch size when compared to the original batch size settings based on **BatchNorm** and **ResNet**. Similar patterns are also observed among other datasets, as shown in Fig. 15.

However, one question may occur: why does batch size matter between 0 and 16? It turns out that although **LayerNorm** can eliminate batch size influence, a **stable loss** still requires a proper batch size. This could also be evident from Fig. 12 in the Google split of the CIFAR warehouse, where the results for batch size 16 surpass the case of batch size 1 by a large gap for uncertainty-based optimization methods (since these methods trying to improve the test-time performance purely by the loss optimization).

Besides, since the batch size is defined to stabilize the loss, we can find some interesting patterns. For example, as shown in Fig. 15, the test sets such as CIFAR-10.1 and CIFAR-10-W show stable performance when batch size varies between 16 and 64. As the source-only performance is already satisfactory, these datasets could be treated as relatively simple tasks. However, large batch size still matters when facing harder cases, as the performance on CIFAR-100-C and ImageNet-C. This verifies the above idea and brings us a new way of setting up a proper batch size when facing different data domains.

As shown in Fig. 16, there is another interesting trend where large batch sizes cannot mitigate the knowledge gap when faced with hard-to-learn corruption domains like Gaussian noise and Shot noise. This highlights the bottleneck in setting batch sizes.

Optimization Layer Matters! As the above experiments were all conducted on top of the **LayerNorm** updating strategy, in this section, we want to examine if **LayerNorm** is inevitable. For better illustration, we summarize the **LayerNorm**-based and full model optimization in Table. 2

To be detailed, we conduct this ablation study mainly on **CoTTA** and **MEMO**. While both **CoTTA** and **MEMO** originally required a full model update in their paper, we would like to examine if updating **LayerNorm** will lead to better adaptation results.

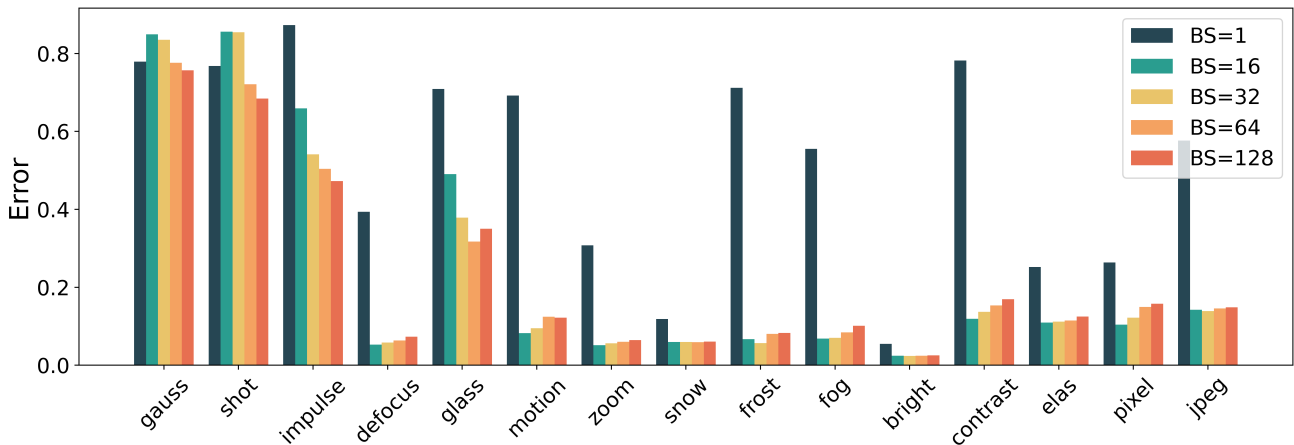


Fig. 16: Impact of varying batch sizes on CIFAR-10-C. The base model is **Tent** optimized on **LayerNorm**.

Table 2: The Comparison of model update strategies across 5 different benchmarks: LayerNorm only v.s. full model. * indicates the variant of COTTA with no parameter reset mechanism.

Method	CIFAR-10-C			CIFAR-10.1			CIFAR-100-C			ImageNet-C			CIFAR-Warehouse		
	LN	ALL	Δ Err	LN	ALL	Δ Err	LN	ALL	Δ Err	LN	ALL	Δ Err	LN	ALL	Δ Err
CoTTA	0.2471	0.5247	-52.91%	0.0750	0.1155	-35.06%	0.4663	0.6442	-27.62%	0.7237	0.8516	-15.02%	0.1823	0.2804	-34.99%
CoTTA*	0.2468	0.7708	-67.98%	0.0750	0.1640	-54.27%	0.4682	0.8961	-47.75%	0.7229	0.9054	-20.16%	0.1820	0.5463	-66.68%
MEMO	0.2116	0.8999	-76.49%	0.0780	0.9000	-91.33%	0.4338	0.9900	-56.18%	0.9032	0.9995	-96.35%	0.1746	0.8955	-80.50%

In our empirical study, we conducted a comprehensive analysis across multiple datasets, including CIFAR-10-C, CIFAR-100-C, ImageNet-C, CIFAR-Warehouse, and CIFAR10.1, to assess the impact of the LayerNorm updating strategy in CoTTA and MEMO models. Notably, for the CIFAR-10-C dataset, we observed a substantial performance improvement of 52.91% when utilizing LayerNorm update compared to updating the entire set of student model parameters. This result underscores the pivotal role of the LayerNorm updating strategy. Similar trends of improved performance were consistently observed in all other datasets, manifesting as Δ Err improvements of 35.06%, 27.62%, 15.02%, and 34.99%, respectively. Remarkably, when examining CoTTA* (CoTTA without parameter reset), we found that updating LayerNorm alone can lead to significant Δ Err improvements.

Furthermore, in the MEMO model, the utilization of the LayerNorm update strategy yielded remarkable enhancements, with the most notable improvement recorded in CIFAR10.1, where the Δ Err demonstrated an impressive 91.33% increase.

In summary, our empirical findings unequivocally demonstrate that the LayerNorm update strategy plays a pivotal and highly beneficial role in ViT-based OTTA methods, showcasing its significance as a critical com-

ponent in enhancing model performance across various datasets.

5 Future Directions

While our initial evaluations shed light on the performance of current OTTA methods using the Vision Transformer (ViT) backbone, it’s evident that many were not tailored explicitly for ViT, resulting in sub-optimal adaptation outcomes. Below, we delineate the attributes of an ideal OTTA for forthcoming research.

- **OTTA for Large-scale Models:** There is a pressing need to explore this avenue further. It necessitates the inception and empirical validation of novel algorithms under standardized benchmarks, constrained batch sizes, and contemporary backbones or expansive pre-trained models. With the emergence of substantial Visual Language Models, such as CLIP, the demand for adapting multi-modal models to specialized datasets exhibiting dynamic shifts may intensify.
- **Hot-swappable OTTA:** Given the rapid evolution of backbone architectures, forthcoming OTTA methods should emphasize extensibility and generalizability in the face of architectural alterations. The crux of the challenge will be devising unsuper-

Table 3: The summary of existing OTTA published in the top-tier conferences before Oct-2023. There are three main categories: data-based, model-based, and optimization-based.

Year	Method	Model-based			Data-based		Optimization-based			
		add.	subst.	prompt	mem.	aug.	loss.	pl.	t-c.	norm.
2021	Tent (Wang et al. 2021)									✓
2021	MixNorm (Hu et al. 2021)		✓							✓
2021	PAD (Wu et al. 2021)		✓			✓		✓		
2021	TTPR (Sivaprasad et al. 2021)					✓				
2021	Core (You et al. 2021)									✓
2021	SLR (Mummadi et al. 2021)	✓					✓			✓
2021	T3A (Iwasawa and Matsuo 2021)		✓		✓					
2022	NOTE (Gong et al. 2022)				✓					✓
2022	EATA (Niu et al. 2022)									✓
2022	CoTTA (Wang et al. 2022a)					✓			✓	
2022	Conjugate PL (Goyal et al. 2022)							✓		
2022	GpreBN (Yang et al. 2022)		✓							✓
2022	CFA (Kojima et al. 2022)									✓
2022	DUA (Mirza et al. 2022)		✓							✓
2022	MEMO (Zhang et al. 2022)					✓	✓			✓
2022	AdaContrast (Chen et al. 2022b)				✓	✓	✓	✓		
2022	TPT (Shu et al. 2022)			✓						
2022	DePT (Gao et al. 2022)			✓						
2023	DN (Gan et al. 2023)			✓						
2023	TAST (Jang et al. 2023)	✓	✓		✓					✓
2023	MECTA (Hong et al. 2023)		✓							✓
2023	DELTA (Zhao et al. 2023a)		✓							✓
2023	TeSLA (Tomar et al. 2023)				✓	✓	✓		✓	
2023	RoTTA (Yuan et al. 2023a)		✓		✓			✓		✓
2023	EcoTTA (Song et al. 2023)	✓						✓		✓
2023	TIPI (Nguyen et al. 2023)					✓				✓
2023	TSD (Wang et al. 2023)		✓		✓		✓			
2023	SAR (Niu et al. 2023)						✓			✓
2023	ECL (Han et al. 2023)				✓			✓		

vised proxies that can aptly simulate prospective, unseen shifts.

– Stable and Robust Optimization for OTTA:

In alignment with our empirical findings, the top-performing methods predominantly leverage the mean teacher architecture or employ a flatness-aware optimizer to effectively tackle a spectrum of distribution shifts. While increasing the batch size offers a partial remedy, this solution isn’t always feasible. Hence, it becomes imperative to formulate strategies that enable a stable and robust gradient descent even with a limited set of unlabeled test samples.

6 Conclusion

Online Test-Time Adaptation (OTTA) has emerged as a crucial area of research in the realm of deep learning. In this paper, we present a comprehensive review of OTTA, offering a detailed explanation of existing methodologies, available datasets, evaluation benchmarks, and practical applications. Additionally, we conduct extensive experiments of the various OTTA methods currently in use, for both effectiveness and efficiency. Drawing from this analysis, we identify several key research challenges that have the potential to shape the future

of OTTA research. We anticipate that this survey will serve as a valuable resource for further exploration.

Data Availability Statement:

The data that support the findings of this study are openly available as summarized in Table 1.

This open-sourced repository will be released and include all the implementation code and experimental configurations of this work.

7 Appendix

Below, we include comprehensive Tables for ImageNet-C and CIFAR-10, including parameter size and amount of trainable parameters for reference.

References

1. L. J. Ba, J. R. Kiros, and G. E. Hinton. Layer normalization. *CoRR*, abs/1607.06450, 2016. URL <http://arxiv.org/abs/1607.06450>.
2. M. Boudiaf, R. Müller, I. B. Ayed, and L. Bertinetto. Parameter-free online test-time adaptation. In *IEEE/CVF Conference on Computer Vision and Pattern Recognition, CVPR 2022, New Orleans, LA, USA, June 18-24, 2022*, pages 8334–8343. IEEE, 2022. doi: 10.1109/CVPR52688.2022.00816. URL <https://doi.org/10.1109/CVPR52688.2022.00816>.

Table 4: The comprehensive table that summarize the OTTA in CIFAR-10-C. The Running time, GLOPs, and Parameter size are provided.

Method	Glass	Fog	Defoc.	Impul.	Contr.	Gauss.	Elastic.	Zoom	Pixel	Frost	Snow	JPEG	Motion	Shot	Brit.	Mean	GFLOPs	#Param (m)	TParam
Source Only	34.60	14.14	12.20	39.47	38.95	60.12	14.70	10.61	25.26	10.39	7.67	16.51	15.30	55.17	3.26	23.89	19.945	269.806	85.654
Batch size = 16																			
Tent	49.02	6.81	5.29	65.93	11.91	84.93	10.96	5.12	10.41	6.68	5.96	14.21	8.25	85.60	2.43	24.90	269.806	85.654	38400
CoTTA-LN	34.50	14.57	12.97	43.96	50.01	58.04	15.05	11.09	22.92	10.43	7.75	16.46	15.92	53.65	3.27	24.71	809.418	256.963	38400
CoTTA-ALL	71.68	51.28	38.25	82.60	79.30	85.57	31.22	16.51	39.95	36.75	37.38	37.37	81.00	88.54	9.72	52.47	809.418	256.963	85654282
CoTTA*-LN	34.58	14.60	13.02	43.71	49.71	58.00	15.03	11.09	22.96	10.45	7.67	16.53	15.93	53.68	3.24	24.68	809.418	256.963	38400
CoTTA*-ALL	77.17	78.07	70.48	85.98	81.41	86.57	74.54	66.80	68.95	78.34	72.30	79.23	79.62	88.83	67.91	77.08	809.418	256.963	85654282
SAR	34.39	14.13	12.18	39.38	34.92	60.67	14.70	10.61	25.17	10.39	7.67	16.51	15.28	55.59	3.26	23.66	539.612	85.654	29184
Conj-CE	61.26	6.36	4.89	80.12	7.94	87.96	10.92	4.20	8.43	5.32	5.33	12.71	7.18	86.63	2.27	26.10	539.612	85.654	38400
MEMO-LN	26.15	9.08	6.17	65.80	9.58	77.68	12.48	5.29	9.14	6.59	5.71	14.45	7.71	59.15	2.49	21.16	809.418	85.654	38400
RoTTA-LN	34.47	13.72	11.70	38.72	37.35	59.55	14.29	10.14	25.38	10.25	7.42	16.31	14.70	54.59	3.07	23.44	269.806	85.654	38400
TAST	81.25	88.58	81.23	83.31	87.40	84.15	78.54	79.59	78.03	81.12	79.51	78.92	81.93	83.55	75.00	81.47	268.445	171.309	85654282
Batch size = 1																			
Tent	70.90	55.50	39.38	87.28	78.20	77.92	25.22	30.77	26.38	71.19	11.85	57.65	69.19	76.82	5.48	52.25	16.863	85.654	38400
CoTTA-LN	34.09	16.63	14.79	43.05	45.14	57.63	15.39	13.23	21.11	10.15	8.25	16.88	17.68	52.36	4.07	24.70	50.589	256.963	38400
CoTTA-ALL	87.81	89.90	86.13	89.17	88.82	89.55	84.91	87.77	86.30	87.42	89.17	88.67	89.06	89.22	81.65	87.70	50.589	256.963	85654282
CoTTA*-LN	35.88	18.35	16.96	46.27	47.31	58.21	17.49	15.12	20.95	10.78	9.60	18.15	19.72	52.15	4.83	26.12	50.589	256.963	38400
CoTTA*-ALL	89.79	89.76	86.30	89.63	89.66	89.78	89.17	89.12	89.32	88.04	89.44	89.18	88.76	89.67	87.83	89.03	50.589	256.963	85654282
SAR	34.63	14.04	12.03	39.55	37.62	61.17	14.63	10.61	24.85	10.38	7.62	16.63	15.20	55.67	3.27	23.86	33.726	85.654	29184
Conj-CE	48.90	55.11	14.09	88.28	84.49	89.11	14.39	29.01	20.95	13.70	27.84	38.25	12.71	88.95	5.43	42.08	33.726	85.654	38400
MEMO LN	85.91	5.55	4.77	87.84	3.76	89.33	11.54	3.70	5.52	4.08	4.36	12.28	6.01	89.32	1.65	27.71	556.475	85.654	38400
RoTTA LN	34.46	13.72	11.71	38.72	37.36	59.55	14.29	10.12	25.39	10.24	7.43	16.32	14.71	54.62	3.07	23.45	16.863	85.654	38400
TAST	81.23	88.59	81.35	83.59	87.76	84.37	78.78	79.32	77.96	81.20	79.61	78.98	82.05	83.63	75.48	81.59	16.778	171.309	85654282

Table 5: The comprehensive table that summarize the OTTA in CIFAR-100-C.

Method	Glass	Fog	Defoc.	Impul.	Contr.	Gauss.	Elastic.	Zoom	Pixel	Frost	Snow	JPEG	Motion	Shot	Brit.	Mean
Source-Only	62.39	34.23	32.01	76.94	60.32	76.05	28.86	25.25	39.73	24.20	19.79	35.62	32.56	72.86	7.32	41.88
Batch size = 16																
Tent	73.69	35.40	16.33	97.06	85.94	91.95	24.4	15.37	26.78	23.54	17.44	33.36	22.09	93.71	5.53	44.17
CoTTA-LN	62.68	41.84	38.77	87.01	74.04	80.53	34.62	30.46	36.46	26.47	22.08	39.70	39.89	77.25	7.58	46.63
CoTTA-ALL	68.75	79.77	45.56	98.58	97.81	94.80	65.83	53.62	38.73	37.63	24.49	67.40	86.00	94.18	13.19	64.42
CoTTA*-LN	63.12	42.25	39.1	87.11	73.93	80.57	34.94	30.71	36.75	26.3	22.42	39.79	40.22	77.47	7.60	46.82
CoTTA*-ALL	91.58	91.85	83.09	98.61	97.91	97.39	91.57	90.03	86.26	83.19	79.11	90.57	93.47	97.00	72.5	89.61
SAR	63.09	31.41	30.72	82.17	64.76	79.59	27.39	24.36	34.76	24.1	19.61	34.01	29.26	77.55	7.32	42.01
Conj-CE	86.24	37.12	13.06	97.87	94.18	97.49	22.73	11.07	18.64	33.83	14.13	31.64	16.06	97.03	4.86	45.06
MEMO LN	83.03	68.62	17.49	96.33	30.39	94.71	25.19	16.58	28.71	19.93	17.13	34.18	20.07	92.96	5.38	43.38
Batch size = 1																

- D. Brahma and P. Rai. A probabilistic framework for life-long test-time adaptation. In *IEEE/CVF Conference on Computer Vision and Pattern Recognition, CVPR 2023, Vancouver, BC, Canada, June 17-24, 2023*, pages 3582–3591. IEEE, 2023. doi: 10.1109/CVPR52729.2023.00349. URL <https://doi.org/10.1109/CVPR52729.2023.00349>.
- T. Campbell and T. Broderick. Bayesian coresets construction via greedy iterative geodesic ascent. In J. G. Dy and A. Krause, editors, *Proceedings of the 35th International Conference on Machine Learning, ICML 2018, Stockholm, Sweden, July 10-15, 2018*, volume 80 of *Proceedings of Machine Learning Research*, pages 697–705. PMLR, 2018. URL <http://proceedings.mlr.press/v80/campbell18a.html>.
- X. Cao and I. W. Tsang. Bayesian active learning by disagreements: A geometric perspective. *CoRR*, abs/2105.02543, 2021. URL <https://arxiv.org/abs/2105.02543>.
- F. M. Carlucci, L. Porzi, B. Caputo, E. Ricci, and S. R. Bulò. Autodial: Automatic domain alignment layers. In *IEEE International Conference on Computer Vision, ICCV 2017, Venice, Italy, October 22-29, 2017*, pages 5077–5085. IEEE Computer Society, 2017. doi: 10.1109/ICCV.2017.542. URL <https://doi.org/10.1109/ICCV.2017.542>.
- M. Caron, H. Touvron, I. Misra, H. Jégou, J. Mairal, P. Bojanowski, and A. Joulin. Emerging properties in self-supervised vision transformers. In *2021 IEEE/CVF International Conference on Computer Vision, ICCV 2021, Montreal, QC, Canada, October 10-17, 2021*, pages 9630–9640. IEEE, 2021. doi: 10.1109/ICCV48922.

- 2021.00951. URL <https://doi.org/10.1109/ICCV48922.2021.00951>.
- D. Chen, D. Wang, T. Darrell, and S. Ebrahimi. Contrastive test-time adaptation. In *IEEE/CVF Conference on Computer Vision and Pattern Recognition, CVPR 2022, New Orleans, LA, USA, June 18-24, 2022*, pages 295–305. IEEE, 2022a. doi: 10.1109/CVPR52688.2022.00039. URL <https://doi.org/10.1109/CVPR52688.2022.00039>.
- D. Chen, D. Wang, T. Darrell, and S. Ebrahimi. Contrastive test-time adaptation. In *Proceedings of the IEEE/CVF Conference on Computer Vision and Pattern Recognition*, pages 295–305, 2022b.
- Y. Chen, E. K. Garcia, M. R. Gupta, A. Rahimi, and L. Cazzanti. Similarity-based classification: Concepts and algorithms. *J. Mach. Learn. Res.*, 10:747–776, 2009. doi: 10.5555/1577069.1577096. URL <https://dl.acm.org/doi/10.5555/1577069.1577096>.
- M. Choi, J. Choi, S. Baik, T. H. Kim, and K. M. Lee. Test-time adaptation for video frame interpolation via meta-learning. *IEEE Transactions on Pattern Analysis and Machine Intelligence*, 44(12):9615–9628, 2021.
- Y. Cui, M. Jia, T. Lin, Y. Song, and S. J. Belongie. Class-balanced loss based on effective number of samples. In *IEEE Conference on Computer Vision and Pattern Recognition, CVPR 2019, Long Beach, CA, USA, June 16-20, 2019*, pages 9268–9277. Computer Vision Foundation / IEEE, 2019. doi: 10.1109/CVPR.2019.00949. URL http://openaccess.thecvf.com/content_CVPR_2019/html/Cui_Class-Balanced_Loss_Based_on_Effective_Number_of_Samples_CVPR_2019_paper.html.

Table 6: The comprehensive table of the OTTA performance on ImageNet-c on ViT base patch16 (224*224)

ImageNet-C	Glass	Fog	Defoc.	Impul.	Contr.	Gauss.	Elastic.	Zoom	Pixel	Frost	Snow	JPEG	Motion	Shot	Brit.	Mean
Source-Only	73.92	63.76	65.54	79.18	89.84	79.88	53.38	62.42	39.26	60.70	63.66	45.06	61.20	77.38	33.38	63.24
Batch size = 16																
Tent	77.86	97.88	73.88	97.24	97.28	95.28	57.54	85.92	33.12	97.64	96.06	42.40	92.60	90.88	29.30	77.66
CoTTA AP	73.72	94.82	92.80	99.14	92.94	99.06	78.06	84.14	79.40	88.92	96.70	54.48	86.58	98.10	58.48	85.16
CoTTA LP	77.06	68.50	75.4	92.10	87.60	92.06	63.28	67.24	50.28	71.36	80.74	52.46	71.58	89.46	46.40	72.37
CoTTA AN	90.30	95.84	95.08	99.28	95.24	99.12	87.9	88.2	90.20	94.84	97.50	68.04	95.82	98.68	62.08	90.54
CoTTA LN	77.26	68.6	75.32	91.58	87.08	92.28	63.3	67.18	50.72	70.74	80.64	52.02	71.48	89.72	46.46	72.29
SAR Ad	52.78	48.34	54.74	71.92	85.74	73.18	37.54	46.48	31.70	61.14	49.24	36.74	48.48	64.92	27.52	52.70
Conjugate PL (CE)	68.30	42.96	76.74	93.70	84.52	96.60	34.46	45.64	31.00	83.90	55.12	35.28	53.32	84.88	28.6	61.00
Conjugate PL (Poly)	68.26	47.48	54.08	93.68	75.82	96.68	34.08	47.42	29.94	81.26	65.06	36.06	68.36	87.7	29.16	61.00
MEMO w LN	96.10	95.62	96.26	98.68	99.18	98.08	97.48	87.80	35.40	93.58	96.30	83.56	94.50	98.26	84.06	90.32
RoTTA	73.50	63.24	65.14	78.40	89.58	79.02	53.10	61.94	39.12	60.34	63.24	44.62	60.80	76.88	33.12	62.80
TAST	99.76	99.64	99.74	99.68	99.90	99.64	99.46	99.30	99.12	99.46	99.32	98.78	99.58	99.36	98.44	99.41
Batch size = 1																
Tent	99.66	99.46	97.90	99.64	99.84	99.80	98.16	98.60	97.56	99.28	97.46	96.90	98.18	99.66	90.34	98.16
CoTTA AP	99.24	99.64	99.06	99.54	99.78	99.80	97.94	99.20	97.48	98.08	99.20	98.60	99.46	99.02	94.82	98.72
CoTTA LP	80.38	69.62	82.82	96.40	90.80	95.30	65.80	67.46	46.52	72.82	81.56	51.42	71.74	93.66	42.28	73.91
CoTTA AN	99.62	99.70	99.54	99.60	99.82	99.80	98.82	99.48	99.30	99.28	99.58	99.20	99.60	99.64	98.70	99.45
CoTTA LN	82.84	72.14	84.56	94.98	92.66	94.66	66.16	70.64	48.88	78.10	83.78	51.62	76.08	91.92	45.12	75.61
SAR Ad	70.58	66.64	72.40	83.60	97.76	82.96	57.54	62.98	41.02	64.54	78.52	46.34	66.96	82.72	37.78	67.49
Conjugate PL (CE)	99.38	96.42	98.18	99.76	99.74	99.76	91.54	96.02	96.74	98.86	97.86	96.90	98.26	99.14	90.38	97.26
MEMO w LN	99.82	99.58	99.78	99.84	99.72	99.90	99.54	99.30	98.04	99.66	99.48	98.46	99.52	99.80	97.30	99.32
RoTTA	73.46	63.26	65.10	78.40	89.58	79.04	53.14	61.94	39.12	60.36	63.18	44.64	60.86	76.88	33.12	62.81
TAST	99.76	99.68	99.70	99.66	99.88	99.64	99.42	99.26	99.18	99.46	99.32	98.74	99.60	99.38	98.42	99.41

- Y. Ding, J. Liang, B. Jiang, A. Zheng, and R. He. Maps: A noise-robust progressive learning approach for source-free domain adaptive keypoint detection. *arXiv preprint arXiv:2302.04589*, 2023.
- A. Dosovitskiy, L. Beyer, A. Kolesnikov, D. Weissenborn, X. Zhai, T. Unterthiner, M. Dehghani, M. Minderer, G. Heigold, S. Gelly, J. Uszkoreit, and N. Houlsby. An image is worth 16x16 words: Transformers for image recognition at scale. In *9th International Conference on Learning Representations, ICLR 2021, Virtual Event, Austria, May 3-7, 2021*. OpenReview.net, 2021. URL <https://openreview.net/forum?id=YicbFdNTTy>.
- P. Foret, A. Kleiner, H. Mobahi, and B. Neyshabur. Sharpness-aware minimization for efficiently improving generalization. In *9th International Conference on Learning Representations, ICLR 2021, Virtual Event, Austria, May 3-7, 2021*. OpenReview.net, 2021. URL <https://openreview.net/forum?id=6TmImposlRM>.
- Y. Gan, Y. Bai, Y. Lou, X. Ma, R. Zhang, N. Shi, and L. Luo. Decorate the newcomers: Visual domain prompt for continual test time adaptation. In B. Williams, Y. Chen, and J. Neville, editors, *Thirty-Seventh AAAI Conference on Artificial Intelligence, AAAI 2023, Thirty-Fifth Conference on Innovative Applications of Artificial Intelligence, IAAI 2023, Thirteenth Symposium on Educational Advances in Artificial Intelligence, EAAI 2023, Washington, DC, USA, February 7-14, 2023*, pages 7595–7603. AAAI Press, 2023. URL <https://ojs.aaai.org/index.php/AAAI/article/view/25922>.
- Y. Gandelsman, Y. Sun, X. Chen, and A. A. Efros. Test-time training with masked autoencoders. In *NeurIPS*, 2022. URL http://papers.nips.cc/paper_files/paper/2022/hash/bcdec1c2d60f94a93b6e36f937aa0530-Abstract-Conference.html.
- Y. Ganin and V. S. Lempitsky. Unsupervised domain adaptation by backpropagation. In F. R. Bach and D. M. Blei, editors, *Proceedings of the 32nd International Conference on Machine Learning, ICML 2015, Lille, France, 6-11 July 2015*, volume 37 of *JMLR Workshop and Conference Proceedings*, pages 1180–1189. JMLR.org, 2015. URL <http://proceedings.mlr.press/v37/ganin15.html>.
- Y. Gao, X. Shi, Y. Zhu, H. Wang, Z. Tang, X. Zhou, M. Li, and D. N. Metaxas. Visual prompt tuning for test-time domain adaptation. *CoRR*, abs/2210.04831, 2022. doi: 10.48550/arXiv.2210.04831. URL <https://doi.org/10.48550/arXiv.2210.04831>.
- T. Gong, J. Jeong, T. Kim, Y. Kim, J. Shin, and S. Lee. NOTE: robust continual test-time adaptation against temporal correlation. In *NeurIPS*, 2022. URL http://papers.nips.cc/paper_files/paper/2022/hash/ae6c7dbd9429b3a75c41b5fb47e57c9e-Abstract-Conference.html.
- S. Goyal, M. Sun, A. Raghunathan, and J. Z. Kolter. Test time adaptation via conjugate pseudo-labels. In *NeurIPS*, 2022. URL http://papers.nips.cc/paper_files/paper/2022/hash/28e9eff897f98372409b40ae1ed3ea4c-Abstract-Conference.html.
- J. Han, L. Zeng, L. Du, W. Ding, and J. Feng. Rethinking precision of pseudo label: Test-time adaptation via complementary learning. *CoRR*, abs/2301.06013, 2023. doi: 10.48550/arXiv.2301.06013. URL <https://doi.org/10.48550/arXiv.2301.06013>.
- K. He, H. Fan, Y. Wu, S. Xie, and R. Girshick. Momentum contrast for unsupervised visual representation learning. In *Proceedings of the IEEE/CVF conference on computer vision and pattern recognition*, pages 9729–9738, 2020.
- D. Hegde, V. Sindagi, V. Kilic, A. B. Cooper, M. Foster, and V. Patel. Uncertainty-aware mean teacher for source-free unsupervised domain adaptive 3d object detection. *arXiv preprint arXiv:2109.14651*, 2021.
- D. Hendrycks and T. G. Dietterich. Benchmarking neural network robustness to common corruptions and surface variations. *arXiv preprint arXiv:1807.01697*, 2018.
- D. Hendrycks, N. Mu, E. D. Cubuk, B. Zoph, J. Gilmer, and B. Lakshminarayanan. Augmix: A simple data processing method to improve robustness and uncertainty. In *8th International Conference on Learning Representations, ICLR 2020, Addis Ababa, Ethiopia, April 26-30, 2020*. OpenReview.net, 2020. URL <https://openreview.net/forum?id=S1gmrxHFvB>.
- J. Hong, L. Lyu, J. Zhou, and M. Spranger. MECTA: memory-economic continual test-time model adaptation.

- In *The Eleventh International Conference on Learning Representations, ICLR 2023, Kigali, Rwanda, May 1-5, 2023*. OpenReview.net, 2023. URL <https://openreview.net/pdf?id=N92hjSf5NNh>.
- X. Hu, M. G. Uzunbas, S. Chen, R. Wang, A. Shah, R. Nevatia, and S. Lim. Mixnorm: Test-time adaptation through online normalization estimation. *CoRR*, abs/2110.11478, 2021. URL <https://arxiv.org/abs/2110.11478>.
- J. Huang, A. J. Smola, A. Gretton, K. M. Borgwardt, and B. Schölkopf. Correcting sample selection bias by unlabeled data. In B. Schölkopf, J. C. Platt, and T. Hofmann, editors, *Advances in Neural Information Processing Systems 19, Proceedings of the Twentieth Annual Conference on Neural Information Processing Systems, Vancouver, British Columbia, Canada, December 4-7, 2006*, pages 601–608. MIT Press, 2006. URL <https://proceedings.neurips.cc/paper/2006/hash/a2186aa7c086b46ad4e8bf81e2a3a19b-Abstract.html>.
- L. Huang, D. Yang, B. Lang, and J. Deng. Decorrelated batch normalization. In *2018 IEEE Conference on Computer Vision and Pattern Recognition, CVPR 2018, Salt Lake City, UT, USA, June 18-22, 2018*, pages 791–800. Computer Vision Foundation / IEEE Computer Society, 2018. doi: 10.1109/CVPR.2018.00089. URL http://openaccess.thecvf.com/content_cvpr_2018/html/Huang_Decorrelated_Batch_Normalization_CVPR_2018_paper.html.
- S. Ioffe. Batch renormalization: Towards reducing mini-batch dependence in batch-normalized models. In I. Guyon, U. von Luxburg, S. Bengio, H. M. Wallach, R. Fergus, S. V. N. Vishwanathan, and R. Garnett, editors, *Advances in Neural Information Processing Systems 30: Annual Conference on Neural Information Processing Systems 2017, December 4-9, 2017, Long Beach, CA, USA*, pages 1945–1953, 2017. URL <https://proceedings.neurips.cc/paper/2017/hash/c54e7837e0cd0ced286cb5995327d1ab-Abstract.html>.
- S. Ioffe and C. Szegedy. Batch normalization: Accelerating deep network training by reducing internal covariate shift. In F. R. Bach and D. M. Blei, editors, *Proceedings of the 32nd International Conference on Machine Learning, ICML 2015, Lille, France, 6-11 July 2015*, volume 37 of *JMLR Workshop and Conference Proceedings*, pages 448–456. JMLR.org, 2015. URL <http://proceedings.mlr.press/v37/ioffe15.html>.
- Y. Iwasawa and Y. Matsuo. Test-time classifier adjustment module for model-agnostic domain generalization. In M. Ranzato, A. Beygelzimer, Y. N. Dauphin, P. Liang, and J. W. Vaughan, editors, *Advances in Neural Information Processing Systems 34: Annual Conference on Neural Information Processing Systems 2021, NeurIPS 2021, December 6-14, 2021, virtual*, pages 2427–2440, 2021. URL <https://proceedings.neurips.cc/paper/2021/hash/1415fe9fea0fa1e45dddcff5682239a0-Abstract.html>.
- M. Jang, S. Chung, and H. W. Chung. Test-time adaptation via self-training with nearest neighbor information. In *The Eleventh International Conference on Learning Representations, ICLR 2023, Kigali, Rwanda, May 1-5, 2023*. OpenReview.net, 2023. URL <https://openreview.net/pdf?id=EzLtB4M1SBM>.
- Y. Kim, J. Yim, J. Yun, and J. Kim. NLNL: negative learning for noisy labels. In *2019 IEEE/CVF International Conference on Computer Vision, ICCV 2019, Seoul, Korea (South), October 27 - November 2, 2019*, pages 101–110. IEEE, 2019. doi: 10.1109/ICCV.2019.00019. URL <https://doi.org/10.1109/ICCV.2019.00019>.
- M. Kimura. Understanding test-time augmentation. In T. Mantoro, M. Lee, M. A. Ayu, K. W. Wong, and A. N. Hidayanto, editors, *Neural Information Processing - 28th International Conference, ICONIP 2021, Sanur, Bali, Indonesia, December 8-12, 2021, Proceedings, Part I*, volume 13108 of *Lecture Notes in Computer Science*, pages 558–569. Springer, 2021. doi: 10.1007/978-3-030-92185-9_46. URL https://doi.org/10.1007/978-3-030-92185-9_46.
- H. Kingetsu, K. Kobayashi, Y. Okawa, Y. Yokota, and K. Nakazawa. Multi-step test-time adaptation with entropy minimization and pseudo-labeling. In *2022 IEEE International Conference on Image Processing, ICIP 2022, Bordeaux, France, 16-19 October 2022*, pages 4153–4157. IEEE, 2022. doi: 10.1109/ICIP46576.2022.9897419. URL <https://doi.org/10.1109/ICIP46576.2022.9897419>.
- T. Kojima, Y. Matsuo, and Y. Iwasawa. Robustifying vision transformer without retraining from scratch by test-time class-conditional feature alignment. In L. D. Raedt, editor, *Proceedings of the Thirty-First International Joint Conference on Artificial Intelligence, IJCAI 2022, Vienna, Austria, 23-29 July 2022*, pages 1009–1016. ijcai.org, 2022. doi: 10.24963/ijcai.2022/141. URL <https://doi.org/10.24963/ijcai.2022/141>.
- A. Krizhevsky, I. Sutskever, and G. E. Hinton. Imagenet classification with deep convolutional neural networks. *Advances in neural information processing systems*, 25, 2012.
- T. Lee, J. Tremblay, V. Blukis, B. Wen, B.-U. Lee, I. Shin, S. Birchfield, I. S. Kweon, and K.-J. Yoon. Tta-cope: Test-time adaptation for category-level object pose estimation. In *Proceedings of the IEEE/CVF Conference on Computer Vision and Pattern Recognition*, pages 21285–21295, 2023.
- Y. Li, N. Wang, J. Shi, J. Liu, and X. Hou. Revisiting batch normalization for practical domain adaptation. In *5th International Conference on Learning Representations, ICLR 2017, Toulon, France, April 24-26, 2017, Workshop Track Proceedings*. OpenReview.net, 2017. URL <https://openreview.net/forum?id=Hk6dkJQFxx>.
- J. Liang, D. Hu, and J. Feng. Do we really need to access the source data? source hypothesis transfer for unsupervised domain adaptation. In *Proceedings of the 37th International Conference on Machine Learning, ICML 2020, 13-18 July 2020, Virtual Event*, volume 119 of *Proceedings of Machine Learning Research*, pages 6028–6039. PMLR, 2020. URL <http://proceedings.mlr.press/v119/liang20a.html>.
- J. Liang, R. He, and T. Tan. A comprehensive survey on test-time adaptation under distribution shifts. *CoRR*, abs/2303.15361, 2023. doi: 10.48550/arXiv.2303.15361. URL <https://doi.org/10.48550/arXiv.2303.15361>.
- H. Liu, Z. Chi, Y. Yu, Y. Wang, J. Chen, and J. Tang. Meta-auxiliary learning for future depth prediction in videos. In *Proceedings of the IEEE/CVF Winter Conference on Applications of Computer Vision*, pages 5756–5765, 2023.
- Y. Luo, Z. Wang, Z. Chen, Z. Huang, and M. Baktashmotlagh. Source-free progressive graph learning for open-set domain adaptation. *IEEE Trans. Pattern Anal. Mach. Intell.*, 45(9):11240–11255, 2023. doi: 10.1109/TPAMI.2023.3270288. URL <https://doi.org/10.1109/TPAMI.2023.3270288>.
- W. Ma, C. Chen, S. Zheng, J. Qin, H. Zhang, and Q. Dou. Test-time adaptation with calibration of medical image classification nets for label distribution shift. In

- International Conference on Medical Image Computing and Computer-Assisted Intervention*, pages 313–323. Springer, 2022.
- R. A. Marsden, M. Döbler, and B. Yang. Gradual test-time adaptation by self-training and style transfer. *CoRR*, abs/2208.07736, 2022. doi: 10.48550/arXiv.2208.07736. URL <https://doi.org/10.48550/arXiv.2208.07736>.
- M. J. Mirza, J. Micorek, H. Possegger, and H. Bischof. The norm must go on: Dynamic unsupervised domain adaptation by normalization. In *IEEE/CVF Conference on Computer Vision and Pattern Recognition, CVPR 2022, New Orleans, LA, USA, June 18-24, 2022*, pages 14745–14755. IEEE, 2022. doi: 10.1109/CVPR52688.2022.01435. URL <https://doi.org/10.1109/CVPR52688.2022.01435>.
- H. B. Mitchell and P. A. Schaefer. A “soft” k-nearest neighbor voting scheme. *International journal of intelligent systems*, 16(4):459–468, 2001.
- C. K. Mummadi, R. Huttmacher, K. Rambach, E. Levinkov, T. Brox, and J. H. Metzen. Test-time adaptation to distribution shift by confidence maximization and input transformation. *arXiv preprint arXiv:2106.14999*, 2021.
- A. T. Nguyen, T. Nguyen-Tang, S.-N. Lim, and P. H. Torr. Tipi: Test time adaptation with transformation invariance. In *Proceedings of the IEEE/CVF Conference on Computer Vision and Pattern Recognition*, pages 24162–24171, 2023.
- S. Niu, J. Wu, Y. Zhang, Y. Chen, S. Zheng, P. Zhao, and M. Tan. Efficient test-time model adaptation without forgetting. In K. Chaudhuri, S. Jegelka, L. Song, C. Szepesvári, G. Niu, and S. Sabato, editors, *International Conference on Machine Learning, ICML 2022, 17-23 July 2022, Baltimore, Maryland, USA*, volume 162 of *Proceedings of Machine Learning Research*, pages 16888–16905. PMLR, 2022. URL <https://proceedings.mlr.press/v162/niu22a.html>.
- S. Niu, J. Wu, Y. Zhang, Z. Wen, Y. Chen, P. Zhao, and M. Tan. Towards stable test-time adaptation in dynamic wild world. In *The Eleventh International Conference on Learning Representations, ICLR 2023, Kigali, Rwanda, May 1-5, 2023*. OpenReview.net, 2023. URL <https://openreview.net/pdf?id=g2YraF75Tj>.
- J. Quinonero-Candela, M. Sugiyama, A. Schwaighofer, and N. D. Lawrence. *Dataset shift in machine learning*. MIT Press, 2008.
- A. Radford, J. W. Kim, C. Hallacy, A. Ramesh, G. Goh, S. Agarwal, G. Sastry, A. Askell, P. Mishkin, J. Clark, G. Krueger, and I. Sutskever. Learning transferable visual models from natural language supervision. In M. Meila and T. Zhang, editors, *Proceedings of the 38th International Conference on Machine Learning, ICML 2021, 18-24 July 2021, Virtual Event*, volume 139 of *Proceedings of Machine Learning Research*, pages 8748–8763. PMLR, 2021. URL <http://proceedings.mlr.press/v139/radford21a.html>.
- B. Recht, R. Roelofs, L. Schmidt, and V. Shankar. Do CIFAR-10 classifiers generalize to cifar-10? *CoRR*, abs/1806.00451, 2018. URL <http://arxiv.org/abs/1806.00451>.
- R. Rombach, A. Blattmann, D. Lorenz, P. Esser, and B. Ommer. High-resolution image synthesis with latent diffusion models. In *Proceedings of the IEEE/CVF Conference on Computer Vision and Pattern Recognition (CVPR)*, pages 10684–10695, June 2022.
- S. Roy, A. Siarohin, E. Sangineto, S. R. Bulò, N. Sebe, and E. Ricci. Unsupervised domain adaptation using feature-whitening and consensus loss. In *IEEE Conference on Computer Vision and Pattern Recognition, CVPR 2019, Long Beach, CA, USA, June 16-20, 2019*, pages 9471–9480. Computer Vision Foundation / IEEE, 2019. doi: 10.1109/CVPR.2019.00970. URL http://openaccess.thecvf.com/content_CVPR_2019/html/Roy_Unsupervised_Domain_Adaptation_Using_Feature-Whitening_and_Consensus_Loss_CVPR_2019_paper.html.
- C. Saltori, E. Krivosheev, S. Lathuilière, N. Sebe, F. Galasso, G. Fiameni, E. Ricci, and F. Poiesi. Gipso: Geometrically informed propagation for online adaptation in 3d lidar segmentation. In *European Conference on Computer Vision*, pages 567–585. Springer, 2022.
- D. Shanmugam, D. W. Blalock, G. Balakrishnan, and J. V. Guttag. Better aggregation in test-time augmentation. In *2021 IEEE/CVF International Conference on Computer Vision, ICCV 2021, Montreal, QC, Canada, October 10-17, 2021*, pages 1194–1203. IEEE, 2021. doi: 10.1109/ICCV48922.2021.00125. URL <https://doi.org/10.1109/ICCV48922.2021.00125>.
- C. E. Shannon. A mathematical theory of communication. *Bell Syst. Tech. J.*, 27(4):623–656, 1948. doi: 10.1002/j.1538-7305.1948.tb00917.x. URL <https://doi.org/10.1002/j.1538-7305.1948.tb00917.x>.
- M. Shu, W. Nie, D. Huang, Z. Yu, T. Goldstein, A. Anandkumar, and C. Xiao. Test-time prompt tuning for zero-shot generalization in vision-language models. In *NeurIPS*, 2022. URL http://papers.nips.cc/paper_files/paper/2022/hash/5bf2b802e24106064dc547ae9283bb0c-Abstract-Conference.html.
- P. T. Sivaprasad et al. Test time adaptation through perturbation robustness. *CoRR*, abs/2110.10232, 2021. URL <https://arxiv.org/abs/2110.10232>.
- J. Song, J. Lee, I. S. Kweon, and S. Choi. Ecotta: Memory-efficient continual test-time adaptation via self-distilled regularization. *CoRR*, abs/2303.01904, 2023. doi: 10.48550/arXiv.2303.01904. URL <https://doi.org/10.48550/arXiv.2303.01904>.
- X. Sun, X. Leng, Z. Wang, Y. Yang, Z. Huang, and L. Zheng. Cifar-10-warehouse: Broad and more realistic testbeds in model generalization analysis. *arXiv preprint arXiv:2310.04414*, 2023.
- Y. Sun, X. Wang, Z. Liu, J. Miller, A. A. Efros, and M. Hardt. Test-time training with self-supervision for generalization under distribution shifts. In *Proceedings of the 37th International Conference on Machine Learning, ICML 2020, 13-18 July 2020, Virtual Event*, volume 119 of *Proceedings of Machine Learning Research*, pages 9229–9248. PMLR, 2020. URL <http://proceedings.mlr.press/v119/sun20b.html>.
- A. Tarvainen and H. Valpola. Mean teachers are better role models: Weight-averaged consistency targets improve semi-supervised deep learning results. In *5th International Conference on Learning Representations, ICLR 2017, Toulon, France, April 24-26, 2017, Workshop Track Proceedings*. OpenReview.net, 2017. URL <https://openreview.net/forum?id=ry8u21rt1>.
- D. Tomar, G. Vray, B. Bozorgtabar, and J. Thiran. Tesla: Test-time self-learning with automatic adversarial augmentation. *CoRR*, abs/2303.09870, 2023. doi: 10.48550/arXiv.2303.09870. URL <https://doi.org/10.48550/arXiv.2303.09870>.
- D. Ulyanov, A. Vedaldi, and V. S. Lempitsky. Instance normalization: The missing ingredient for fast stylization. *CoRR*, abs/1607.08022, 2016. URL <http://arxiv.org/abs/1607.08022>.

- D. Wang, E. Shelhamer, S. Liu, B. A. Olshausen, and T. Darrell. Tent: Fully test-time adaptation by entropy minimization. In *9th International Conference on Learning Representations, ICLR 2021, Virtual Event, Austria, May 3-7, 2021*. OpenReview.net, 2021. URL <https://openreview.net/forum?id=uX13bZLkr3c>.
- M. Wang and W. Deng. Deep visual domain adaptation: A survey. *Neurocomputing*, 312:135–153, 2018. doi: 10.1016/j.neucom.2018.05.083. URL <https://doi.org/10.1016/j.neucom.2018.05.083>.
- Q. Wang, O. Fink, L. V. Gool, and D. Dai. Continual test-time domain adaptation. In *IEEE/CVF Conference on Computer Vision and Pattern Recognition, CVPR 2022, New Orleans, LA, USA, June 18-24, 2022*, pages 7191–7201. IEEE, 2022a. doi: 10.1109/CVPR52688.2022.00706. URL <https://doi.org/10.1109/CVPR52688.2022.00706>.
- S. Wang, D. Zhang, Z. Yan, J. Zhang, and R. Li. Feature alignment and uniformity for test time adaptation. *CoRR*, abs/2303.10902, 2023. doi: 10.48550/arXiv.2303.10902. URL <https://doi.org/10.48550/arXiv.2303.10902>.
- Z. Wang, M. Ye, X. Zhu, L. Peng, L. Tian, and Y. Zhu. Metateacher: Coordinating multi-model domain adaptation for medical image classification. *Advances in Neural Information Processing Systems*, 35:20823–20837, 2022b.
- Y. Wen, D. Tran, and J. Ba. Batchensemble: an alternative approach to efficient ensemble and lifelong learning. In *8th International Conference on Learning Representations, ICLR 2020, Addis Ababa, Ethiopia, April 26-30, 2020*. OpenReview.net, 2020. URL <https://openreview.net/forum?id=Sk1f1yrYDr>.
- Q. Wu, X. Yue, and A. Sangiovanni-Vincentelli. Domain-agnostic test-time adaptation by prototypical training with auxiliary data. In *NeurIPS 2021 Workshop on Distribution Shifts: Connecting Methods and Applications*, 2021.
- Y. Wu and K. He. Group normalization. *Int. J. Comput. Vis.*, 128(3):742–755, 2020. doi: 10.1007/s11263-019-01198-w. URL <https://doi.org/10.1007/s11263-019-01198-w>.
- J. Yang, X. Meng, and M. W. Mahoney. Implementing randomized matrix algorithms in parallel and distributed environments. *Proc. IEEE*, 104(1):58–92, 2016. doi: 10.1109/JPROC.2015.2494219. URL <https://doi.org/10.1109/JPROC.2015.2494219>.
- T. Yang, S. Zhou, Y. Wang, Y. Lu, and N. Zheng. Test-time batch normalization. *CoRR*, abs/2205.10210, 2022. doi: 10.48550/arXiv.2205.10210. URL <https://doi.org/10.48550/arXiv.2205.10210>.
- F. You, J. Li, and Z. Zhao. Test-time batch statistics calibration for covariate shift. *CoRR*, abs/2110.04065, 2021. URL <https://arxiv.org/abs/2110.04065>.
- L. Yuan, B. Xie, and S. Li. Robust test-time adaptation in dynamic scenarios. In *IEEE/CVF Conference on Computer Vision and Pattern Recognition, CVPR 2023, Vancouver, BC, Canada, June 17-24, 2023*, pages 15922–15932. IEEE, 2023a. doi: 10.1109/CVPR52729.2023.01528. URL <https://doi.org/10.1109/CVPR52729.2023.01528>.
- L. Yuan, B. Xie, and S. Li. Robust test-time adaptation in dynamic scenarios. *CoRR*, abs/2303.13899, 2023b. doi: 10.48550/arXiv.2303.13899. URL <https://doi.org/10.48550/arXiv.2303.13899>.
- M. Zhang, S. Levine, and C. Finn. MEMO: test time robustness via adaptation and augmentation. In *NeurIPS*, 2022. URL http://papers.nips.cc/paper_files/paper/2022/hash/fc28053a08f59fccb48b11f2e31e81c7-Abstract-Conference.html.
- B. Zhao, C. Chen, and S. Xia. Delta: Degradation-free fully test-time adaptation. In *The Eleventh International Conference on Learning Representations, ICLR 2023, Kigali, Rwanda, May 1-5, 2023*. OpenReview.net, 2023a. URL <https://openreview.net/pdf?id=eGm22rqG93>.
- H. Zhao, Y. Liu, A. Alahi, and T. Lin. On pitfalls of test-time adaptation. In A. Krause, E. Brunskill, K. Cho, B. Engelhardt, S. Sabato, and J. Scarlett, editors, *International Conference on Machine Learning, ICML 2023, 23-29 July 2023, Honolulu, Hawaii, USA*, volume 202 of *Proceedings of Machine Learning Research*, pages 42058–42080. PMLR, 2023b. URL <https://proceedings.mlr.press/v202/zhao23d.html>.
- K. Zhou, Z. Liu, Y. Qiao, T. Xiang, and C. C. Loy. Domain generalization: A survey. *IEEE Trans. Pattern Anal. Mach. Intell.*, 45(4):4396–4415, 2023. doi: 10.1109/TPAMI.2022.3195549. URL <https://doi.org/10.1109/TPAMI.2022.3195549>.